NASA TN D-1942

NASA TN D-1942

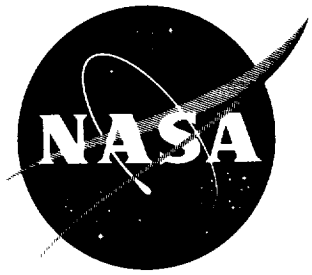

TECHNICAL NOTE

D-1942

APPLICATION OF DORODNITSYN'S INTEGRAL METHOD TO NONEQUILIBRIUM FLOWS OVER POINTED BODIES

By Jerry C. South, Jr.

Langley Research Center
Langley Station, Hampton, Va.

NATIONAL AERONAUTICS AND SPACE ADMINISTRATION
WASHINGTON

August 1963

NATIONAL AERONAUTICS AND SPACE ADMINISTRATION

TECHNICAL NOTE D-1942

APPLICATION OF DORODNITSYN'S INTEGRAL METHOD TO NONEQUILIBRIUM FLOWS OVER POINTED BODIES

By Jerry C. South, Jr.

SUMMARY

Dorodnitsyn's integral method is used to obtain an approximate solution to the supersonic nonequilibrium flow over pointed bodies with attached shock waves. The partial differential equations governing the flow are converted to an approximate set of ordinary equations, which are solved by numerical integration starting at the body tip.

Detailed analytical and numerical results for the first approximation are presented, considering the vibrational relaxation of a diatomic gas over a wedge or cone. It is shown that the first approximation yields:

(1) The exact flow-variable gradients at the wedge tip

(2) Expressions for the flow-variable gradients at the cone tip which are in agreement with extrapolations of characteristics calculations

(3) A good approximate algebraic solution for frozen or equilibrium conical flow

(4) An approximate expression for the nonequilibrium-flow stream function which affords a means of obtaining variations across the shock layer of the temperature and vibrational energy.

Numerical results for both the wedge and cone compare favorably with identical cases computed by the method of characteristics.

INTRODUCTION

At present there is considerable interest in the real gas effects associated with the strong shock waves and extreme temperatures characteristic of hypersonic flow. Such phenomena as molecular vibration, dissociation, electronic excitation, ionization, and radiation may occur and may cause large deviations from ideal-gas aerodynamic behavior. In addition, a further complication is introduced when the flow is not in thermodynamic equilibrium. An essential feature

common to all nonequilibrium flows is the entropy change along streamlines; thus the temperature, density, pressure, and velocity cannot be simply related along a given streamline.

In flows which are entirely supersonic, the method of characteristics is available for exact numerical results. Sedney et al. (ref. 1) have calculated the supersonic nonequilibrium flow over a wedge by consideration of vibrational relaxation in pure nitrogen. They noted, however, evidence of certain difficulties which do not appear in similar ideal-gas calculations. First-order calculations were found to be inadequate, while second-order results depended quite critically on grid size. A judicious choice of dependent variables was necessary to insure success in any case. Some added difficulties appeared when the procedure was extended to nonequilibrium flow past a cone (ref. 2).

Flows with imbedded subsonic regions (mixed flows), such as the supersonic blunt-body problem, have been calculated by various means. Comprehensive surveys of the blunt-body problem can be found in references 3 and 4. One of the methods most frequently employed for calculating frozen or equilibrium blunt-body flows is the inverse method (ref. 3), which starts with an assumed shock-wave shape and finally results in a determination of the corresponding body shape. Lick (refs. 5 and 6) used this method to calculate a nonequilibrium blunt-body flow, in which vibrational relaxation and dissociation in oxygen and nitrogen were considered. He also noted certain stability and convergence difficulties, apparently more severe than in frozen-flow calculations and dependent on grid size. Finally it is worthwhile to note that the inverse method cannot be carried far into the supersonic region of a blunt body (ref. 3), regardless of the thermodynamics, and a changeover to the method of characteristics is necessary in order to obtain results somewhat downstream of the sonic line.

In view of the problems associated with these methods in the calculation of nonequilibrium flows, it is desirable to investigate other techniques which are more straightforward and which are readily adaptable to high-speed computing. In 1958, A. A. Dorodnitsyn (ref. 7) described a method of integral relations which has been used on a variety of classical aerodynamic problems. This method not only has the above-mentioned advantages but can be continued into the supersonic region of mixed-flow problems (ref. 8) with certain restrictions (ref. 9). In supersonic-flow problems involving a shock layer, the Nth integral approximation is briefly outlined as follows: the region between the body surface and the shock wave is divided into N equal (for simplicity) strips. The governing partial differential equations are then cast into a "divergence" form and integrated, from the surface to the boundary of each strip, over the coordinate normal to the surface. The result is N integro-differential equations to replace each original partial differential equation. To arrive at the final approximating set of ordinary differential equations, Nth-degree polynomials are used for the integrands of any appearing integrals. More specific details of this general procedure can be found in references 4, 7, and 10. The results of references 7 and 10 indicated that in the ideal-gas mixed-flow problems studied, the convergence of the method was rapid; the numerical results of the second approximation differed little from those of the third. Traugott (refs. 8 and 11) demonstrated that even the first approximation was surprisingly accurate for the ideal-gas, supersonic, blunt-body problem.

Although the usefulness and versatility of the technique have been demonstrated previously in ideal-gas, mixed-flow problems (refs. 7, 10, 11, and 12), t has not yet been established that the method is applicable to nonequilibrium lows. The results of such an application are reported in the present paper. etailed analytical and numerical results using the first approximation are preented for the vibrationally relaxing flow of a pure diatomic gas past wedges nd cones. Not only are these two shapes of classical interest in gas dynamics, ut their use affords a direct comparison with results obtained in more exact nalyses (refs. 1 and 2).

The author is indebted to R. Sedney and N. Gerber of the Ballistics Research aboratories, Aberdeen Proving Ground, for assistance rendered during the formative stages of this work and for extensive characteristics calculations supplied or direct comparison with the present results.

SYMBOLS

p frozen-flow specific heat at constant pressure

vibrational energy

eq equilibrium vibrational energy

$= p + \rho u^2$

$= p + \rho v^2$

$= \rho v$

0 or 1 for plane or axisymmetric flow

frozen-flow Mach number, $\frac{V}{\sqrt{\gamma p/\rho}}$

pressure

gas constant

radial coordinate normal to axis of symmetry

temperature

$= \rho u$

$,v$ velocity components in x and y directions, respectively

total velocity

x,y coordinates along and normal to body surface

$z = \rho uv$

β shock-wave angle, measured counterclockwise from free-stream directio

γ ratio of frozen-flow specific heats

δ shock-layer thickness in y-direction

ϵ vibrational driving force, $\frac{E_{eq} - E}{\tau}$

Θ_v characteristic vibrational temperature

θ wedge or cone half-angle

λ shock-layer included angle, $\beta - \theta$

ρ density

τ vibrational relaxation time

$\phi = \delta/x$

ψ stream function

ω flow-deflection angle behind shock wave

Subscripts:

∞ free-stream quantity

0 quantity evaluated at surface ($y = 0$)

δ quantity evaluated at shock wave ($y = \delta$)

x=0 quantity evaluated at $x = 0$

Primed quantities are dimensional; unprimed quantities are dimensionless, as shown immediately preceding and after equations (1) to (6).

Barred quantities are corrected surface flow variables.

ANALYSIS

Basic Equations and Definitions

The theoretical model used in this paper is that of the steady, inviscid, isoenergetic flow of a pure diatomic gas. The relaxation of the molecular vibrations is assumed to be the only dissipative mechanism in the flow. This model is identical to that of references 1 and 2 and thereby affords a direct comparison of the present results with the more exact calculations of those references. Although it is relatively simple, the present model has most of the essential features of isoenergetic nonequilibrium flows; namely, entropy production along streamlines, an added term (the vibrational energy) in the ideal-gas energy equation, and a rate equation to describe the approach to equilibrium of the additional degree of freedom. The perfect-gas equation of state is used.

The governing partial differential equations are written in a body-oriented coordinate system, with x,y the coordinates along and normal to the body surface. In the cases to be studied the approach to equilibrium is quite rapid, so that the region of interest is confined to a small area in the shock layer near the body tip. The characteristic time scale is thus chosen to be the vibrational relaxation time just behind the shock wave at the body tip, $\tau'_{\delta,x=0}$. The characteristic length is $V'_\infty \tau'_{\delta,x=0}$. In general, the relaxation time is a function of temperature and pressure, and in references 1 and 2 this variation was approximated by

$$\tau' \propto \frac{\left[\exp(C/T')^{1/3}\right]}{p'}$$

where the constant C was determined from experimental data. Reference 1 demonstrated that the variable relaxation time produced only a secondary effect in the numerical results; that is, the approach to equilibrium was somewhat retarded, but all variables reached the same asymptotes as those for τ' = Constant. The experimental constant C is another initial parameter for a given numerical example, and to simplify the problem, the assumption is made for the present that $\tau' = \tau'_{\delta,x=0}$ = Constant.

In dimensionless form the basic equations are as follows, with $j = 0$ or 1 for plane or axisymmetric flow:

Continuity:

$$\frac{\partial}{\partial x}(\rho u r^j) + \frac{\partial}{\partial y}(\rho v r^j) = 0 \tag{1}$$

x-momentum:

$$u \frac{\partial u}{\partial x} + v \frac{\partial u}{\partial y} + \frac{1}{\rho} \frac{\partial p}{\partial x} = 0 \tag{2}$$

y-momentum:

$$u \frac{\partial v}{\partial x} + v \frac{\partial v}{\partial y} + \frac{1}{\rho} \frac{\partial p}{\partial y} = 0 \tag{3}$$

Rate:

$$u \frac{\partial E}{\partial x} + v \frac{\partial E}{\partial y} - \epsilon = 0 \tag{4}$$

Energy:

$$T + E + \frac{\gamma - 1}{2} M_\infty{}^2 V^2 = 1 + \frac{\gamma - 1}{2} M_\infty{}^2 \tag{5}$$

State:

$$\gamma M_\infty{}^2 p = \rho T \tag{6}$$

Because the present paper is especially concerned with the flow past wedges and cones, terms arising due to body curvature are omitted in equations (1) to (4). The inclusion of these terms presents no added difficulty, and the extension of the present work to arbitrary smooth pointed shapes is a simple matter.

The reference velocity, temperature, and density are V_∞', T_∞', and ρ_∞', respectively. The reference pressure is $\rho_\infty' V_\infty'^2$, while the vibrational energy is referred to $c_p' T_\infty'$. The rate equation (4) is that used by Bethe and Teller (ref. 13) and also in references 1 and 2. The quantity ϵ is a "driving force" given as

$$\epsilon = \frac{E_{eq} - E}{\tau} \tag{7}$$

where E_{eq} is the vibrational energy that the flow would have locally if it were in thermodynamic equilibrium and is taken to be, as in references 1 and 2,

$$E_{eq} = \frac{2}{7} \Theta_v \left[\exp\left(\frac{\Theta_v}{T}\right) - 1 \right]^{-1} \tag{8}$$

The equilibrium vibrational energy E_{eq} is then a function of only the local temperature, and Θ_v is the characteristic vibrational temperature, a constant for any particular gas, referenced to T_∞'. The factor 2/7 is the ratio R'/c_p' for an ideal diatomic gas ($\gamma = 7/5$).

The geometry and coordinate system for a cone are illustrated in figure 1.

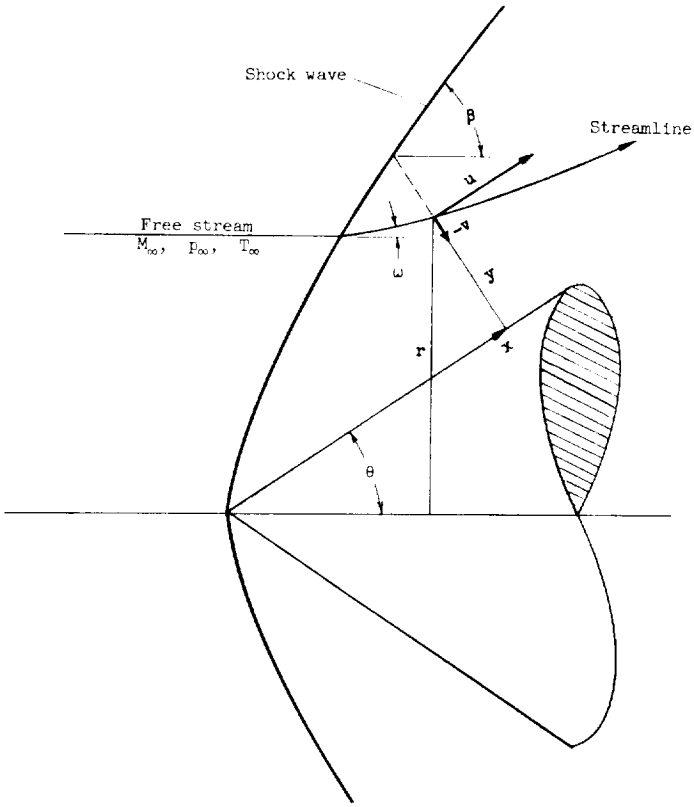

Figure 1.- Geometry and coordinate system (cone illustrated).

Divergence form.- The notation of references 10 and 11 is convenient for use in defining the following quantities:

$$\left.\begin{aligned} t &= \rho u \\ h &= \rho v \\ z &= \rho uv \\ g &= p + \rho u^2 \\ H &= p + \rho v^2 \end{aligned}\right\} \qquad (9)$$

After each of equations (2), (3), and (4) is multiplied by ρr^j, and when the continuity equation and the derivative chain-rule together with the definitions (eqs. (9)) are used, equations (1) to (4) can be written as follows:

$$\frac{\partial}{\partial x}\left(tr^j\right) + \frac{\partial}{\partial y}\left(hr^j\right) = 0 \qquad (10)$$

$$\frac{\partial}{\partial x}\left(gr^j\right) + \frac{\partial}{\partial y}\left(zr^j\right) - jp \sin\theta = 0 \qquad (11)$$

$$\frac{\partial}{\partial x}\left(zr^j\right) + \frac{\partial}{\partial y}\left(Hr^j\right) - jp \cos\theta = 0 \qquad (12)$$

$$\frac{\partial}{\partial x}\left(tEr^j\right) + \frac{\partial}{\partial y}\left(hEr^j\right) - \rho\epsilon r^j = 0 \qquad (13)$$

where $r = x \sin\theta + y \cos\theta$ for the cone. This form of the equations is sometimes referred to as the divergence or conservation form. It is a basic step in the method of integral relations, affording a straightforward procedure for converting the partial differential equations to an approximate ordinary set.

Conversion of Equations to Ordinary Differential Equations

With equations (10) to (13) written in the convenient divergence form, they can be converted to an approximate set of ordinary differential equations by integration over the variable y, so that x is left as the single independent variable. (The equations could be integrated over x, with y as the single independent variable. The geometry and coordinate system suggest, however, that the present procedure will give the best results.) As mentioned in the "Introduction," the method consists of N approximations, with the shock layer divided into N equal strips.

First (one-strip) approximation.- In this analysis, only the first approximation, in which the entire region between the shock wave and body surface is treated as a single strip, is considered. Equations (10) to (13) are integrated from $y = 0$ to $y = \delta$, with linear profiles being used for all integrands. The following boundary conditions are used:

At $y = 0$,

$$v_0 = h_0 = z_0 = 0 \tag{14a}$$

At $y = \delta$,

$$E_\delta = 0 \tag{14b}$$

The first condition states that the wedge or cone surface is a streamline, while the second states that the flow is frozen across the shock wave. The temperature ahead of the shock wave is assumed to be such that the free-stream vibrational energy is negligible, or $E_\infty = E_\delta = 0$. From the shock-wave geometry, it can be seen that

$$\frac{d\delta}{dx} = \tan \lambda \tag{15}$$

where $\lambda = \beta - \theta$. When equations (14a), (14b), and (15) are used, the integration of equations (10) to (13) yields the following ordinary equations:

$$x\phi \frac{dt_0}{dx} + x\phi(1 + j\phi \cot \theta)\frac{dt_\delta}{dx} + (\tan \lambda + j\phi)t_0 - (\tan \lambda - j\phi)t_\delta + 2(1 + j\phi \cot \theta)h_\delta = 0 \tag{16}$$

$$x\phi \frac{dg_0}{dx} + x\phi(1 + j\phi \cot \theta)\frac{dg_\delta}{dx} + (\tan \lambda + j\phi)g_0 - (\tan \lambda - j\phi)g_\delta + 2(1 + j\phi \cot \theta)z_\delta - j\phi(p_\delta + p_0) = 0 \tag{17}$$

$$x\phi(1 + j\phi \cot \theta)\frac{dz_\delta}{dx} - (\tan \lambda - j\phi)z_\delta + 2(1 + j\phi \cot \theta)H_\delta$$

$$- 2p_0 - j\phi \cot \theta\left(p_\delta + p_0\right) = 0 \tag{18}$$

$$x\phi \frac{d}{dx}\left(t_0 E_0\right) + (\tan \lambda + j\phi)t_0 E_0 - x\phi\left[\rho_0 \epsilon_0 + (1 + j\phi \cot \theta)\rho_\delta \epsilon_\delta\right] = 0 \tag{19}$$

where $\phi = \delta/x$. The steps necessary in arriving at equations (16) to (19) are given in appendix A.

Equations (16), (17), and (18) are valid, within the first approximation, regardless of the thermodynamic behavior of the gas (frozen, equilibrium, or nonequilibrium flow). They express the conservation of mass and momentum, and no form of the energy equation (5) or equation of state (6) has yet been used. Equation (19) is specifically for nonequilibrium flow; for frozen flow $\tau' = \infty$ and thus $E = 0$ throughout the shock layer. On the other hand, for equilibrium flow, $\tau' = 0$ and $E(x',y') = E_{eq}(x',y')$, and the rate equation is indeterminate. In this latter case, the proper differential equation for E is:

$$u \frac{\partial E}{\partial x'} + v \frac{\partial E}{\partial y'} = \frac{I}{2}\left(E_{eq}\right)^2 \frac{e^{\Theta_v/T}}{T^2}\left(u \frac{\partial T}{\partial x'} + v \frac{\partial T}{\partial y'}\right) \tag{20}$$

and the length scale $V_\infty{}'\tau'_{\delta,x=0}$ is no longer appropriate.

Before the nonequilibrium-flow calculations are attempted, it is convenient to study the special cases of frozen or equilibrium flow by use of equations (16) through (18). In the case of the wedge, the complete exact solution is obtained merely by solving the appropriate (frozen or equilibrium) shock-wave relations. The cone solution is more difficult and is discussed in the following section.

Frozen or Equilibrium Flow Past a Cone

In the study of the steady, inviscid, frozen or equilibrium flow past a cone, there is no length scale. Similarity considerations yield exact, nonlinear, ordinary, differential equations which must be solved numerically. In this section algebraic expressions are derived and give an approximate solution for frozen or equilibrium cone flow.

In this case the shock wave must be straight and flow properties are constant along the cone surface. Then for all values of x,

$$\phi = \tan \lambda \tag{21}$$

and

$$\frac{df_0}{dx} = \frac{df_\delta}{dx} = 0 \tag{22}$$

where f_0 and f_δ represent any function at the cone surface and just behind the shock wave, respectively. Using equations (21) and (22) in equations (16), (17), and (18), and setting $j = 1$ yields the following expressions:

$$t_0 + (\cot \lambda + \cot \theta)h_\delta = 0 \tag{23}$$

$$2u_0t_0 + 2(\cot \lambda + \cot \theta)u_\delta h_\delta + \left(p_0 - p_\delta\right) = 0 \tag{24}$$

$$2(\cot \lambda + \cot \theta)v_\delta h_\delta - (2 \cot \lambda + \cot \theta)\left(p_0 - p_\delta\right) = 0 \tag{25}$$

If $p_0 - p_\delta$ is eliminated from equations (24) and (25) and equation (23) is used in that result the following relation is obtained:

$$u_0 = u_\delta + \frac{v_\delta}{2 \cot \lambda + \cot \theta} \tag{26}$$

The use of the appropriate (frozen or equilibrium) shock-wave relations, the energy equation (5), and the equation of state (6), together with equations (23), (25), and (26), allows a complete solution of the problem.

Again it should be recalled that equations (23) to (26) are valid within the first integral approximation, not only for frozen flow but also for full equilibrium flow, including chemical reactions and ionization. The particular thermodynamic model enters the solution by use of the proper energy equation, equation of state, and shock relations. It is interesting to note that the assumption of isentropic flow was not necessary.

Chushkin and Shchennikov (ref. 14) used the method of integral relations to calculate ideal-gas flows past cones without axial symmetry. They arrived at an algebraic solution for circular cones at zero incidence similar to the one derive in this section, with the following differences. In reference 14 spherical-polar coordinates were used, and the isentropic law ($p \propto \rho^\gamma$) was used in place of the momentum equation along rays. In the present paper, the isentropic law is not contained in the system of equations, and because the solution is approximate, it is not exactly satisfied even in the special cases of frozen or equilibrium flow. Instead, the x-momentum is approximately conserved throughout the shock layer, so that equation (24) results. Although the present approach and that of reference 14 agree numerically at the higher Mach numbers, the present method gives closer agreement to the exact solution in the lower Mach number range. The comparison seems to indicate that the present method yields a more uniform approximation for all of the flow variables.

In figures 2 and 3 the present results ($\gamma = 1.4$, diatomic gas) are compared with exact results from the charts of reference 15 ($\gamma = 1.405$, air) for fully frozen flow past a cone. In figure 2 the shock-wave angle is plotted against the cone angle for a range of free-stream Mach numbers from 1.05 to 10. Also shown in this figure are three points from reference 14 for $M_\infty = 2.0$. The present results are found to be somewhat better than those of reference 14 at this Mach number. Figure 3 shows the variation of cone-surface pressure coefficient with cone angle for the same Mach number range. It can be seen that the equations derived in this section are exact in the limit of zero cone angle; that is, as $\theta \to 0$, $\beta \to \sin^{-1}(1/M_\infty)$, or the shock wave becomes a Mach wave. The overall agreement between the present solution and exact calculations for frozen flow is good, particularly at the higher Mach numbers.

Since the approximate solution for vibrational equilibrium flow is more involved than for frozen flow, details of the method are given in appendix B. In reference 16 some exact calculations were presented for vibrational equilibrium flow of air and nitrogen past cones. Three cases for nitrogen from this reference were chosen for comparison with computations by the present method. The results are shown in table I.

TABLE I.- VIBRATIONAL EQUILIBRIUM FLOW OF NITROGEN PAST A CONE

$[T_\infty' = 300^\circ$ K; $\Theta_v = 11.12$; $\omega = 30$ deg$]$

M_∞	Method*	β, deg	θ, deg	u_0	p_0	T_0	ρ_0
8	Present	38.155	33.943	0.79059	0.34041	5.3460	5.7055
	Exact	38.155	33.972	0.79047	0.34052	5.3481	5.7050
10	Present	37.159	33.475	0.80025	0.32650	7.3055	6.2569
	Exact	37.159	33.499	0.80017	0.32659	7.3073	6.2570
12	Present	36.568	33.196	0.80593	0.31847	9.6320	6.6656
	Exact	36.568	33.216	0.80586	0.31854	9.6339	6.6658

*For present method, see appendix B; for exact method, see reference 16.

The results in this table reveal that for the cases illustrated, the present approximate method agrees with the exact calculations within 0.1 percent. The algebraic equations derived in this section for frozen or equilibrium flow past a cone are special cases of the differential equations (16) to (19). The excellent agreement with exact calculations allows some confidence in proceeding to the case of nonequilibrium flow.

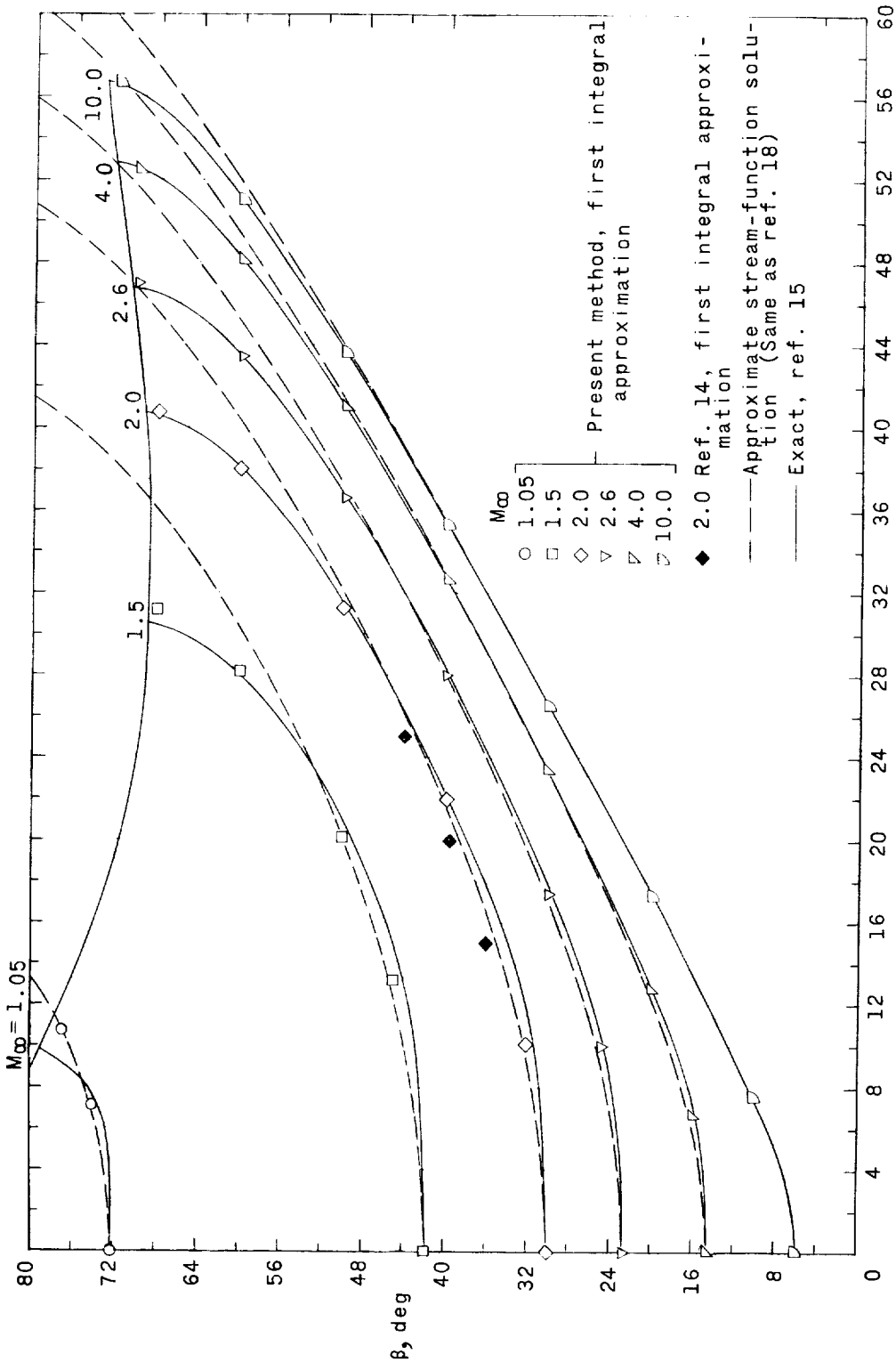

Figure 2.- Shock-wave angle as function of cone angle, frozen flow over a cone.

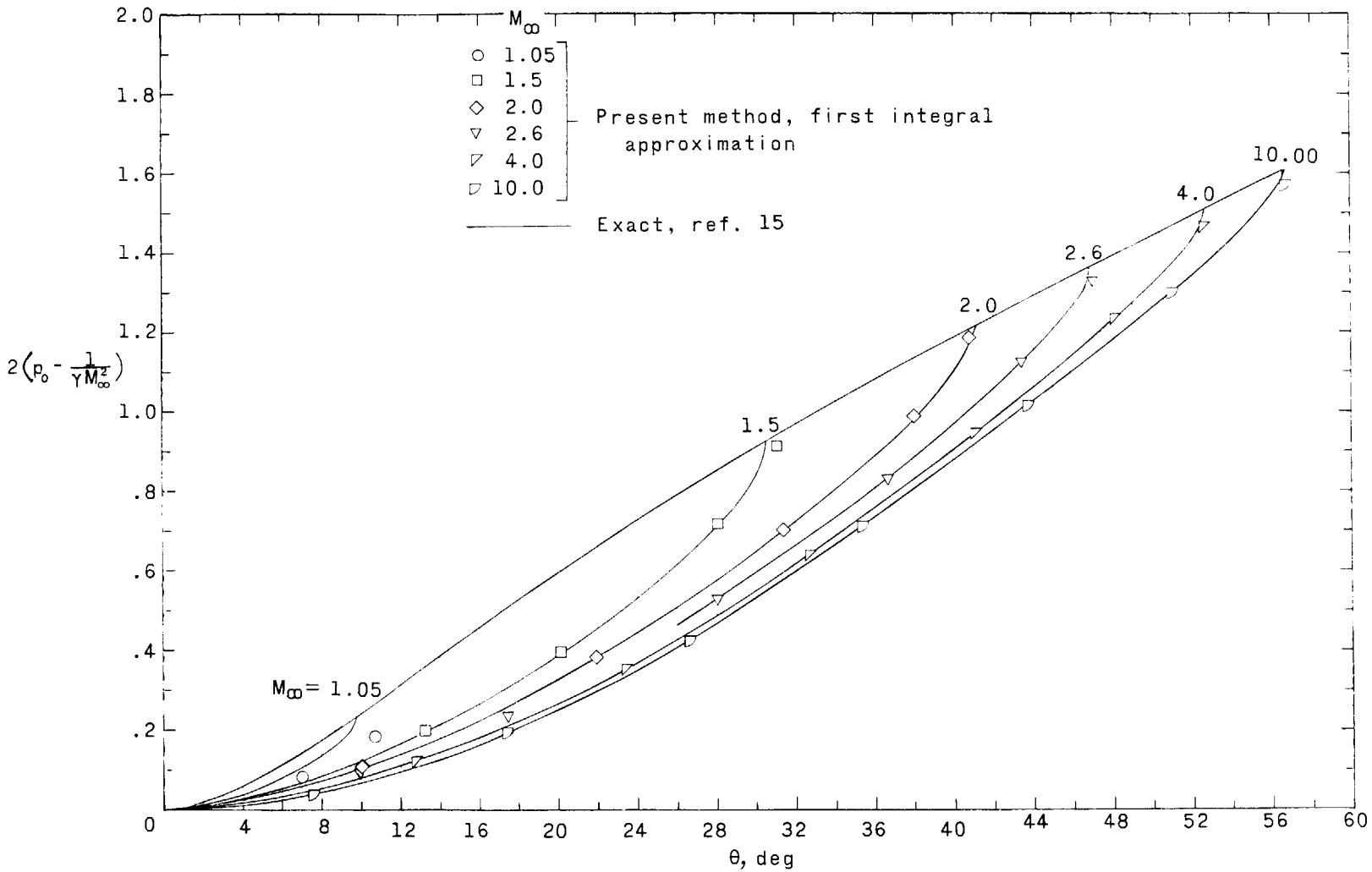

Figure 3.- Surface pressure coefficient as function of cone angle, frozen flow over a cone.

Nonequilibrium Flow Past Wedges and Cones

In the case of nonequilibrium flow past a wedge or a cone, the attached shock wave is curved and the flow variables undergo rapid changes both in the shock layer and along the surface. In order to obtain the shock-wave shape and the variation of properties along the surface, equations (16) to (19) must be presented in a calculable form. This result is accomplished by returning to the original variables β, u_0, p_0, and E_0. Combining the x-derivatives of the energy equation (5), the equation of state (6), and the appropriate definitions of equations (9) provide the following relations:

$$u_0 \frac{dt_0}{dx} = \gamma M_0^2 \frac{dp_0}{dx} + \frac{u_0 t_0}{T_0} \frac{dE_0}{dx} + \left[1 + (\gamma - 1)M_0^2\right] t_0 \frac{du_0}{dx} \tag{27}$$

$$\frac{dg_0}{dx} = \left(1 + \gamma M_0^2\right)\frac{dp_0}{dx} + \frac{u_0 t_0}{T_0} \frac{dE_0}{dx} + \left[2 + (\gamma - 1)M_0^2\right] t_0 \frac{du_0}{dx} \tag{28}$$

It is also recognized that $f_\delta = f_\delta\left[\beta(x)\right]$, where f_δ is again any shock-wave function, so that

$$\frac{df_\delta}{dx} = \frac{df_\delta}{d\beta} \frac{d\beta}{dx} \tag{29}$$

With the use of equations (27) to (29), equations (16) to (19) can be written as follows:

$$A_{11} \frac{dp_0}{dx} + A_{12} \frac{dE_0}{dx} + A_{13} \frac{du_0}{dx} + A_{14} \frac{d\beta}{dx} = K_1 \tag{30}$$

$$A_{21} \frac{dp_0}{dx} + A_{22} \frac{dE_0}{dx} + A_{23} \frac{du_0}{dx} + A_{24} \frac{d\beta}{dx} = K_2 \tag{31}$$

$$A_{34} \frac{d\beta}{dx} = K_3 \tag{32}$$

$$A_{41} \frac{dp_0}{dx} + A_{42} \frac{dE_0}{dx} + A_{43} \frac{du_0}{dx} = K_4 \tag{33}$$

The coefficients A and the nonhomogeneous terms K are listed in appendix C. The necessary frozen shock-wave relations are given in appendix D.

Initial values and derivatives.- Before equations (30) to (33) can be numerically integrated, the initial values of the variables and their derivatives at $x = 0$ must be obtained. In order that the derivatives in equations (30) to (33) be finite at $x = 0$, it is necessary that K_1 to K_4 be finite. In appendix C

it can be seen that K_1, K_2, and K_3 will be indeterminate for the wedge ($j = 0$), if $f_0 = f_\delta$, and will be indeterminate for the cone ($j = 1$), if equations (23), (24), and (25) are satisfied. With the initial condition, at $x = 0$,

$$E_0 = 0 \tag{34}$$

K_4 is also indeterminate. Since the frozen shock-wave equations are used (see the boundary condition (14b)), the existence of frozen flow throughout the shock layer at the tip of the wedge or cone is required.

The initial derivatives can be found by resolving the indeterminate forms of the values of K. The results for the wedge are:

$$\left(\frac{d\beta}{dx}\right)_{x=0} = -J \tag{35}$$

$$\left(\frac{dp_0}{dx}\right)_{x=0} = -J\,\frac{dp_\delta}{d\beta} \tag{36}$$

$$\left(\frac{du_0}{dx}\right)_{x=0} = \frac{1}{t_0}\,\frac{dp_\delta}{d\beta}\,J \tag{37}$$

$$\left(\frac{dE_0}{dx}\right)_{x=0} = \frac{\epsilon_0}{u_0} \tag{38}$$

where

$$J = t_0\,\frac{\epsilon_0}{T_0}\left[\left(M_0^2 - 1\right)\frac{dp_\delta}{d\beta} + t_0 \cot\lambda\,\frac{dv_\delta}{d\beta}\right]^{-1} \tag{39}$$

It can be verified that the foregoing expressions for the wedge tip gradients are the same as the exact expressions derived in reference 17. This result is to be expected, since all the flow variables in the wedge shock layer are constant at the frozen tip, as mentioned before. Then the linear profiles assumed in arriving at equations (30) to (33) are indeed exact at the wedge tip.

The initial derivatives for the cone are similarly found to be

$$\left(\frac{d\beta}{dx}\right)_{x=0} = -\left(\frac{K}{L}\right)(2 \cot\lambda + \cot\theta) \tag{40}$$

$$\left(\frac{dp_0}{dx}\right)_{x=0} = -\left(\frac{K}{L}\right)F_3 \tag{41}$$

$$\left(\frac{du_0}{dx}\right)_{x=0} = \left(\frac{K}{L}\right)\frac{1}{t_0}\left[\frac{2}{3}F_3 - (2\cot\lambda + \cot\theta)(F_1 - F_2)\right] \tag{42}$$

$$\left(\frac{dE_0}{dx}\right)_{x=0} = K\frac{T_0}{u_0 t_0} \tag{43}$$

where the symbols K, L, F_1, F_2, and F_3 are defined in appendix E. Equations (40) to (43) cannot be compared with exact analytical expressions for the cone tip gradients, since none exist (ref. 17). The initial derivatives of β and p_0 calculated with equations (40) and (41) were, however, found to be in excellent agreement with extrapolations (to $x = 0$) of characteristics calculations (ref. 2). The calculation of supersonic flow over a pointed axisymmetric shape by the method of characteristics must be initiated at $x > 0$, since the Mach line characteristic equations have a singularity at $x = 0$. In reference 2 a small but finite frozen region was assumed at the cone tip, and the calculation was started at the downstream boundary of this region. The comparisons for the derivatives of u_0 and E_0 were not so good, and this discrepancy suggested a reexamination of equations (30) to (33) before proceeding further.

Improvement for first approximation.- Since the surface of the wedge or cone is a streamline, equations (2) and (4) can be applied at $y = 0$ (where $v_0 = 0$), yielding for all x:

$$\frac{du_0}{dx} = -\frac{1}{t_0}\frac{dp_0}{dx} \tag{44}$$

and

$$\frac{dE_0}{dx} = \frac{\epsilon_0}{u_0} \tag{45}$$

However, the solution of equations (30) to (33) for the individual derivatives does not give such concise results. The surface velocity gradient is not simply related to the pressure gradient as in equation (44), and dE_0/dx depends not only on ϵ_0 but also on ϵ_δ. This discrepancy is caused by the averaging process of the integral method, and the resulting numerical errors should diminish as higher approximations (two or more strips) are applied. An immediate improvement for the first approximation can be made, however, by properly incorporating equations (44) and (45) in the calculation. This operation is accomplished by defining new variables on the surface, $\bar{u}_0$, $\bar{E}_0$, $\bar{T}_0$, and $\bar{\rho}_0$, as follows:

$$\frac{d\bar{u}_0}{dx} = -\frac{1}{\bar{t}_0}\frac{dp_0}{dx} \tag{46}$$

$$\frac{d\bar{E}_0}{dx} = \frac{\bar{\epsilon}_0}{\bar{u}_0} \tag{47}$$

$$\bar{T}_0 = 1 + \frac{\gamma - 1}{2} M_\infty^2 - \left(\bar{E}_0 + \frac{\gamma - 1}{2} M_\infty^2 \bar{u}_0^2 \right) \tag{48}$$

$$\bar{\rho}_0 = \frac{\gamma M_\infty^2 p_0}{\bar{T}_0} \tag{49}$$

where

$$\bar{t}_0 = \bar{\rho}_0 \bar{u}_0 \tag{50}$$

$$\bar{\epsilon}_0 = \bar{E}_{eq,0} - \bar{E}_0 \tag{51}$$

$$\bar{E}_{eq,0} = \frac{2}{7} \Theta_v \left[\exp\left(\frac{\Theta_v}{\bar{T}_0} \right) - 1 \right]^{-1} \tag{52}$$

Equations (46) to (52) then give improved distributions $\bar{u}_0$, $\bar{E}_0$, etc. which are consistent on the surface with the x-momentum equation, the surface-streamline rate equation, and the pressure distribution obtained from the system of equations (5), (6), (7), (8), and (30) to (33). These barred quantities are referred to as corrected variables. The same corrections can be applied to higher approximations.

Flow details and stream function.- A possible objection to the use of the method of integral relations for calculating nonequilibrium flows is that the linear profiles of the first approximation (see appendix A) do not give realistic flow details between the shock wave and the surface. For this purpose the stream function, defined to satisfy identically the continuity equation (1), is introduced. Then

$$\left.\begin{aligned} tr^j &= \frac{\partial \psi}{\partial y} \\ hr^j &= -\frac{\partial \psi}{\partial x} \end{aligned}\right\} \tag{53}$$

Along lines x = Constant,

$$\psi = \int_0^y tr^j \, dy \tag{54}$$

Then, if the linear profiles consistent with the first approximation are used in equation (54),

$$\frac{\psi}{\delta t_0 (x \sin\theta)^j} = \frac{y}{\delta} + \frac{1}{2}\left[(1 + j\phi \cot\theta)\frac{t_\delta}{t_0} - 1\right]\left(\frac{y}{\delta}\right)^2 \tag{55}$$

Once the surface variables and shock-wave geometry are obtained as functions of x by numerical integration, the x,y coordinates of a streamline ψ = Constant can be determined from equation (55). The first integral-approximation streamline pattern for nonequilibrium flow is thus obtained. If it were desired to obtain the shock-layer details, the equations of motion written in natural coordinates (ref. 17) could be applied along the streamlines to calculate the flow properties at points between the shock wave and the surface. However, this procedure is considered too sophisticated for the first approximation, and a simpler method can be used for the present problem of vibrational relaxation.

First, the accuracy of equation (55) should be examined for cases of frozen or equilibrium flow. As mentioned in a previous section, the shock wave is straight and the flow variables on the surface are constant on both the wedge and cone. Then equation (21) is valid for all values of x; and for the wedge ($j = 0$), $t_0 = t_\delta$, and the streamlines are seen to be straight lines parallel to the surface. For the cone ($j = 1$) equation (23) is used for t_0, and the streamlines are

$$\psi = t_0 \sin\theta xy - \frac{1}{2} t_0 \sin\theta\left(\frac{u_\delta}{v_\delta} + \cot\lambda\right)y^2 \tag{56}$$

Since the coefficients of xy and y^2 are constants, equation (56) is a family of hyperbolas, a result obtained by Hord (ref. 18) in another approximate solution. In order to determine the orientation and asymptotes of the hyperbolas, the axes are rotated to transform equation (56) to normal form; that is, the mixed-product (xy) term is eliminated. This procedure reveals that the hyperbolas have their line of centers normal to the cone axis at the tip and that the cone surface is an asymptote. Furthermore, when the mixed-product coefficient is required to vanish, it is found that

$$\cot 2\theta = \frac{1}{2}\left(\frac{u_\delta}{v_\delta} + \cot\lambda\right) \tag{57}$$

Substituting from appendix D the frozen shock-wave relations (D3) and (D4) into equation (57) allows considerable simplification, so that:

$$\sin^2\theta = \frac{2}{\gamma + 1}\left(\sin^2\beta - \frac{1}{M_\infty^2}\right) \tag{58}$$

This approximate solution for the frozen-flow cone angle is seen to be identical to that obtained in reference 18 by a somewhat different approach. Equation (58) is illustrated graphically in figure 2, and it can be seen that although the numerical accuracy of equation (58) is not good except in the region $M_\infty > 2$, $\beta < 50^\circ$, the simple functional relation has much of the character of the exact solution. Equation (58) is exact in the limit $\theta \to 0$. It appears then that the stream function given by equation (55) may be used to obtain some first-approximation shock-layer profiles in nonequilibrium flows past wedges and cones.

Reference 1 gives a good approximate algebraic solution based on the assumptions that V, τ, and dE_{eq}/dT are constants along a given streamline and equal to their respective frozen-flow values. Then equations (4) and (5) can be solved in closed form. This solution gives the local temperature and vibrational energy at any point on a streamline in terms of the distance traveled along that streamline and the frozen-flow conditions at the point of entry through the shock wave. Equation (55) gives the value of any entering streamline ($y = \delta$) at any station x and at any later station x determines the y coordinate of that streamline. Knowledge of the shock-wave geometry $\beta(x)$ and $\delta(x)$, together with $\bar{t}_0(x)$ (using the corrected value of $\bar{t}_0$) completes the information necessary to construct profiles of T and E at any station x on the wedge or the cone.

RESULTS AND DISCUSSION

The complete shock-wave shape and distributions of flow variables along the surface were obtained by programing the system of equations (5), (6), (7), (8), and (30) to (33), together with the frozen shock-wave relations given in appendix D, on the IBM 7090 electronic data processing system. Equations (46) to (52) were also programed to obtain the corrected surface variables, $\bar{u}_0$, $\bar{E}_0$, $\bar{T}_0$, and $\bar{\rho}_0$. The machine program was given j, M_∞, $\beta_{x=0}$, and Θ_v as initial parameters.

One case each for the wedge and cone was chosen to compare with the previous calculations of references 1 and 2. In these references, the published results accounted for a variation in the vibrational relaxation time, $\tau(p,T)$, whereas in the present investigation, τ is assumed to be constant. The authors of reference 2 (Sedney and Gerber of the Ballistics Research Laboratory, Aberdeen Proving Ground) kindly recomputed these cases for both the wedge and cone with constant τ, which allows a direct evaluation of the present results. These cases were as follows, both for nitrogen ($T_\infty' = 300^\circ$ K, $\Theta_v = 11.12$):

(1) Wedge: $j = 0$, $M_\infty = 6$, $\beta_{x=0} = 57.24^\circ$ (ref. 1)

(2) Cone: $j = 1$, $M_\infty = 12$, $\beta_{x=0} = 53.23^\circ$ (ref. 2)

The results for the first case, for a wedge angle $\theta = 40.024^\circ$, are illustrated in figure 4. In figure 4(a) the shock-wave shape, $\beta(x)$, and the surface pressure distribution, $p_0(x)$, as given by the present first integral approximation

are represented by the solid curves. The corresponding constant τ characteristics results obtained by Sedney and Gerber are indicated by the circles. Figures 4(b) and 4(c) show the surface variables $E_0(x)$, $u_0(x)$, $T_0(x)$, and $\rho_0(x)$. The dashed curves in these figures show the distributions obtained without correction, while the solid curves are the corrected variables obtained from equations (46) to (52). The same breakdown and description applies to figure 5 for the cone, where again the circles represent constant τ characteristics calculations. For illustration, the reference 2 results for the cone pressure for variable τ are also shown in figure 5(a).

It can be seen from figures 4 and 5 that although the present method does not give the correct asymptotes for large x, the error is not great. In references 1 and 2 it was demonstrated that β and p_0 approached the equilibrium values given by the wedge or cone similarity solutions. The shock-wave angle β approached the limit monotonically from above for both the wedge and cone, as did the pressure on the wedge surface. The cone surface pressure in reference 2 overexpanded and slowly approached its equilibrium value from below. In the present calculations the cone surface pressure reaches a minimum at about $x = 3$ and then starts increasing, but the change is so gradual that it cannot be observed on the scale of figure 5(a).

The surface flow variables E_0, u_0, T_0, and ρ_0 do not approach their equilibrium-similarity values for either the wedge or cone because of the existence of an entropy layer adjacent to the surface (refs. 1 and 2), which is caused primarily by the steeper initial shock-wave angle at the tip. The present corrected distributions of these variables is seen to be a considerable improvement on the method. As the dashed curves reveal, these variables undergo an unrealistic overshoot which is necessary in order for $p_0(x)$ and $\beta(x)$ to level off at large x. The vibrational driving force at the shock wave, ϵ_δ, is always nonzero and positive, with nearly the same magnitude for all values of x. In order for all derivatives to tend toward zero as x increases, the driving force at the wall, ϵ_0, ultimately becomes negative to counter the positive ϵ_δ. If a negative ϵ_0 is to be obtained, E_0 must overshoot its local equilibrium value, $E_{eq,0}$. This feature of the first integral approximation was verified by imposing a lower limit on ϵ_0 $(\epsilon_0 \geqq 0)$ in the numerical example shown in figure 4. As expected, all variables, including β and p_0, continued to decrease (or increase) without bound as x increased. In higher integral approximations (two, three, or more strips) the shock-wave driving force ϵ_δ would receive less weight in the resulting system of differential equations, so that the present corrections might not be necessary. (The driving forces ϵ_δ and ϵ_0 appear in the expression K_4 (eq. (33)), which is defined in equation (C16) of appendix C. Note that ϵ_δ has the coefficient $(1 + j\phi \cot \theta)\rho_\delta$, whereas ϵ_0 has the coefficient ρ_0 alone.)

The initial behavior of the present solution, with the proper corrections, is seen to be quite good for all of the variables, and is particularly valuable

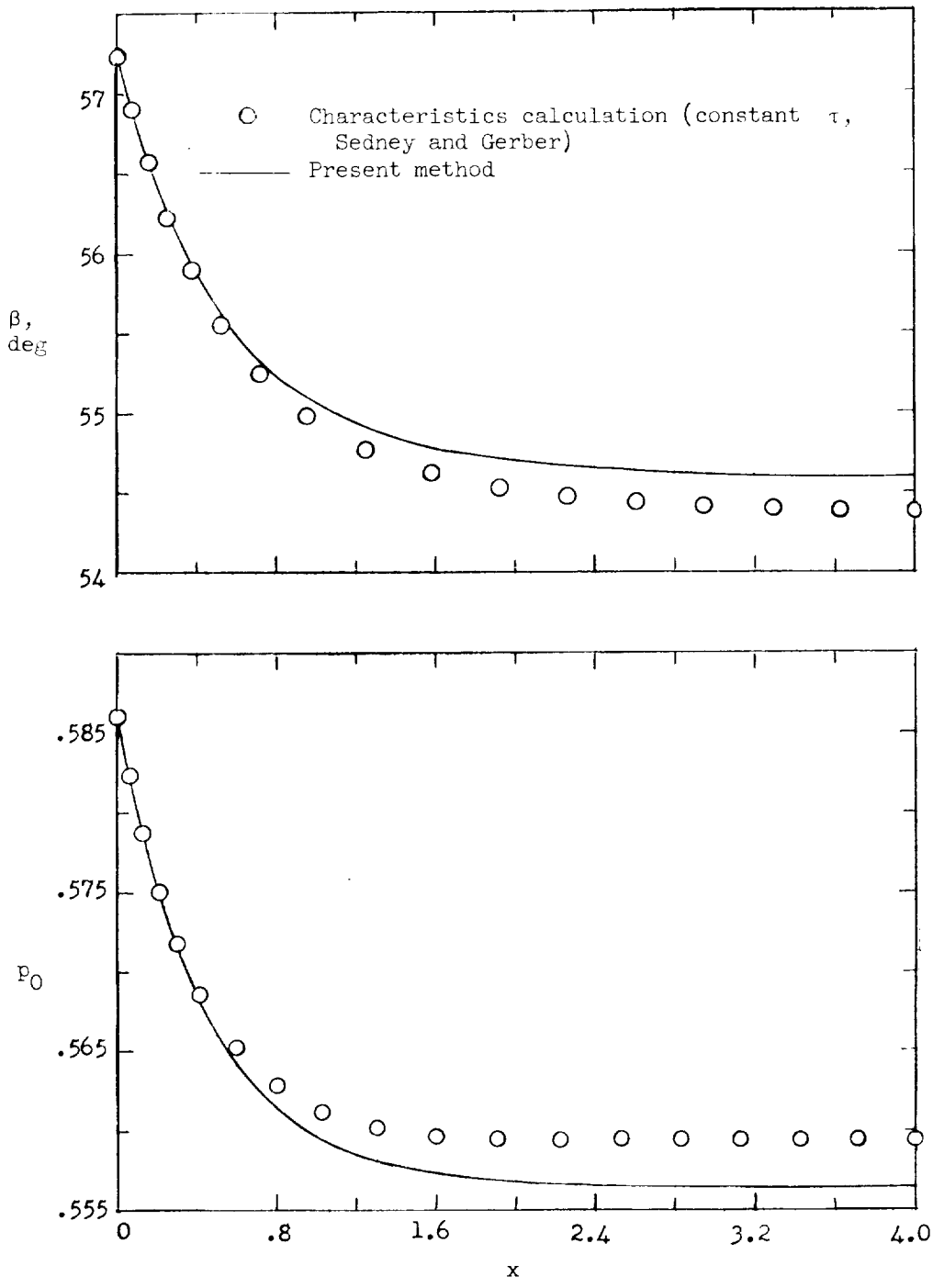

(a) Shock-wave angle and surface pressure as function of x.

Figure 4.- Nonequilibrium vibrational flow over a wedge. $M_\infty = 6$; $\theta = 40.024^\circ$; $\Theta_v = 11.12$ (nitrogen, $T_\infty' = 300^\circ$ K).

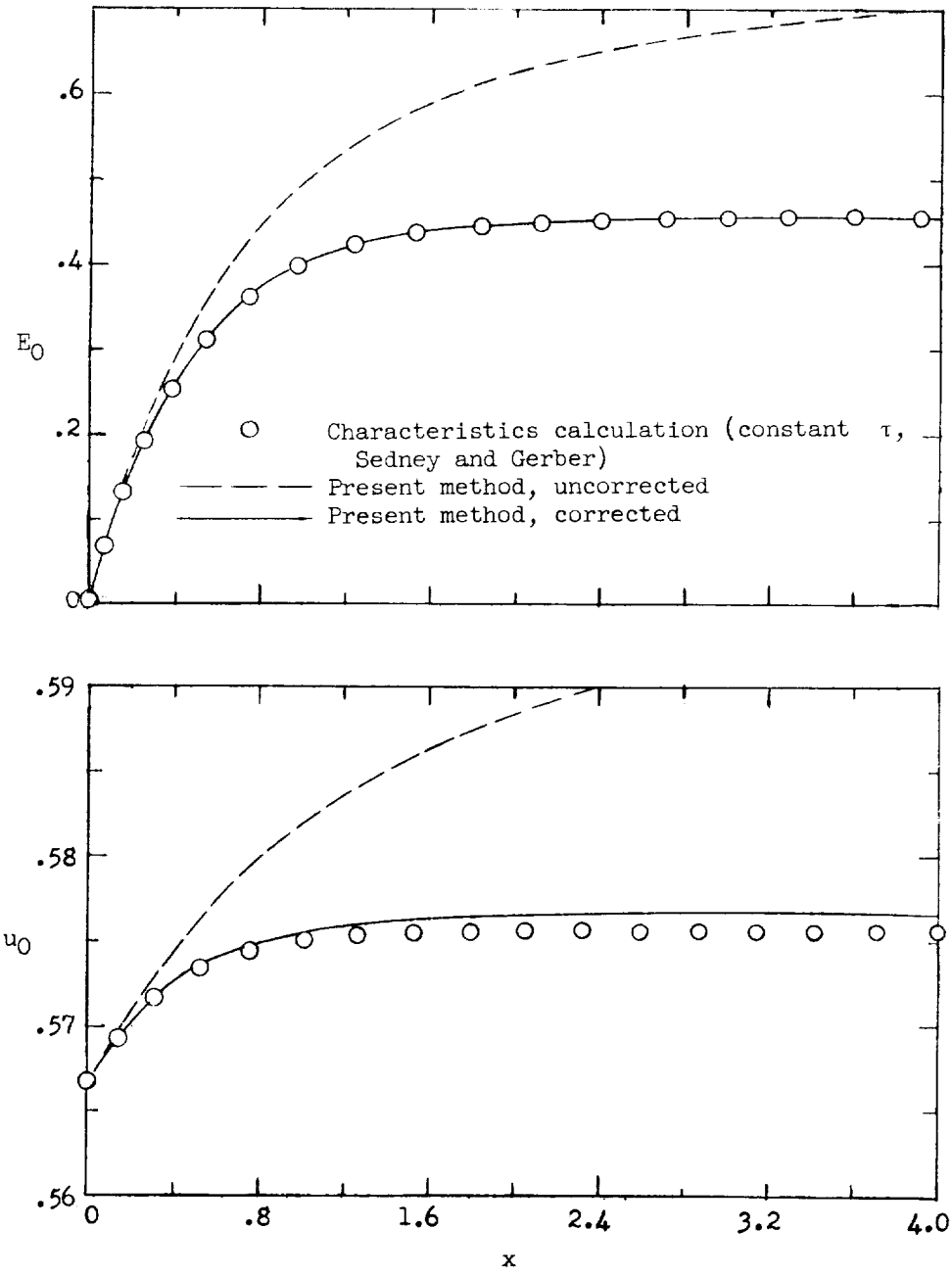

(b) Vibrational energy and velocity on surface as function of x.

Figure 4.- Continued.

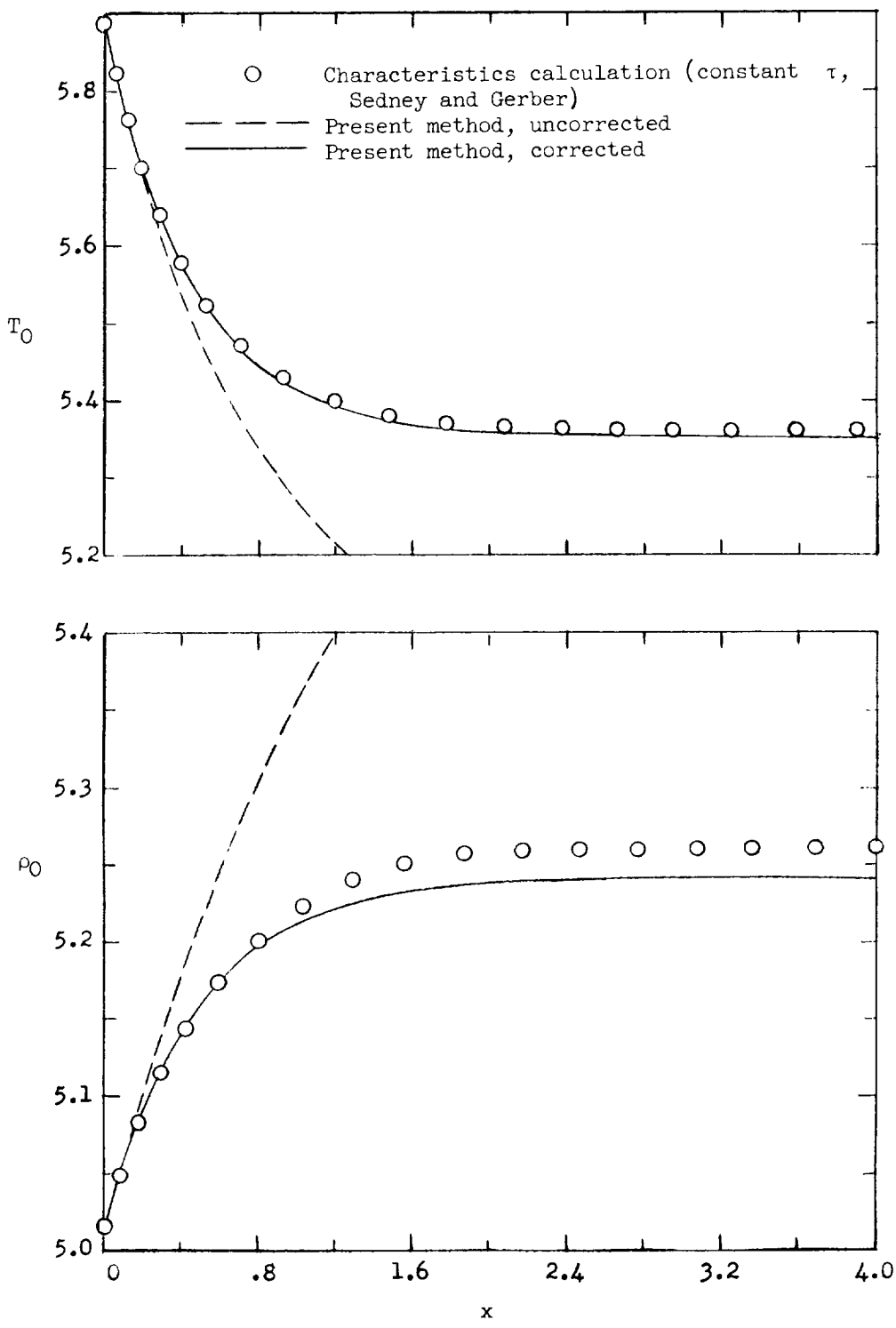

(c) Temperature and density on the surface as function of x.

Figure 4.- Concluded.

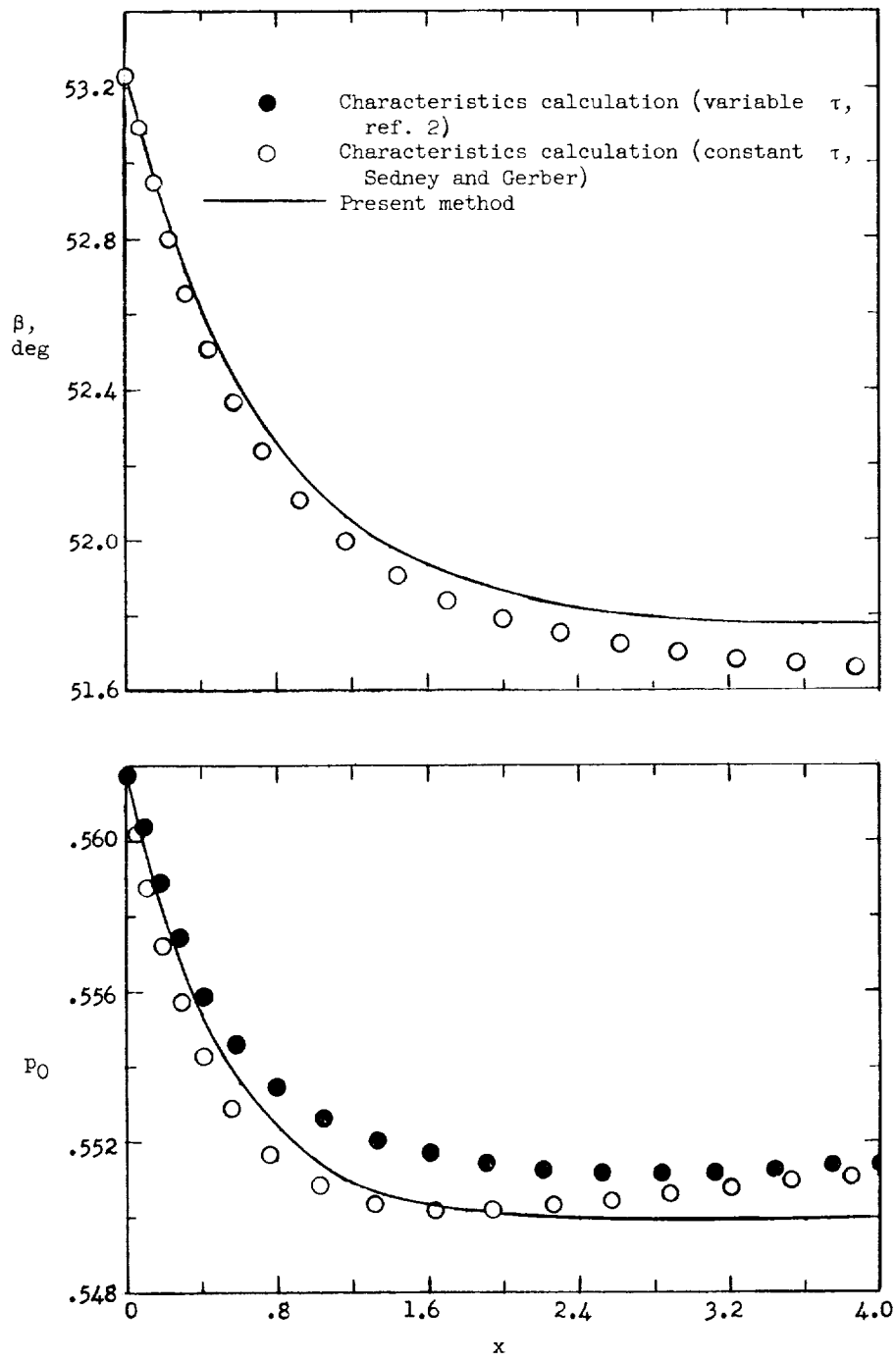

(a) Shock-wave angle and surface pressure as function of x.

Figure 5.- Nonequilibrium vibrational flow over a cone. $M_\infty = 12$; $\theta = 46.358^\circ$; $\Theta_v = 11.12$ (nitrogen, $T_\infty' = 300^\circ$ K).

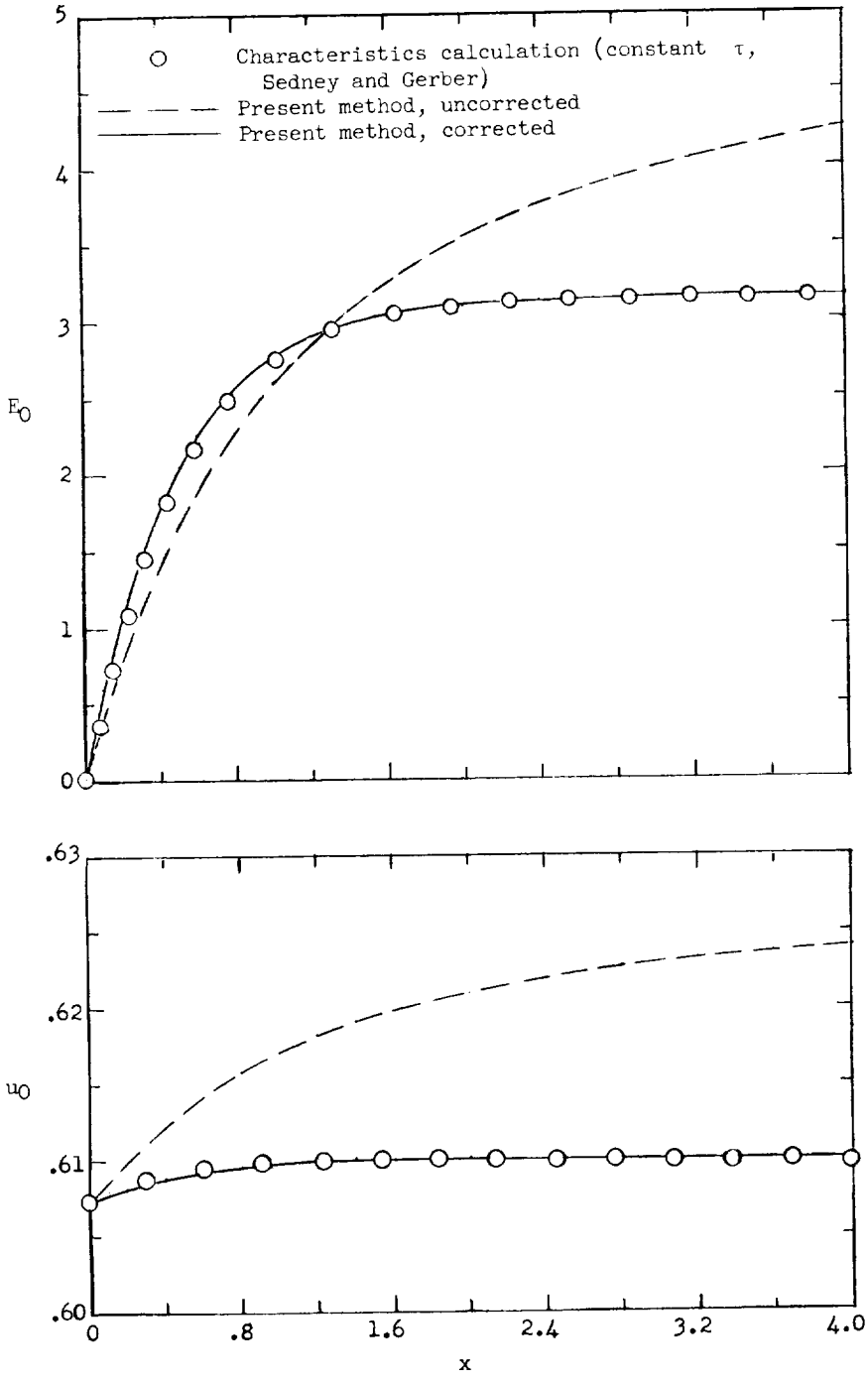

(b) Vibrational energy and velocity on surface.

Figure 5.- Continued.

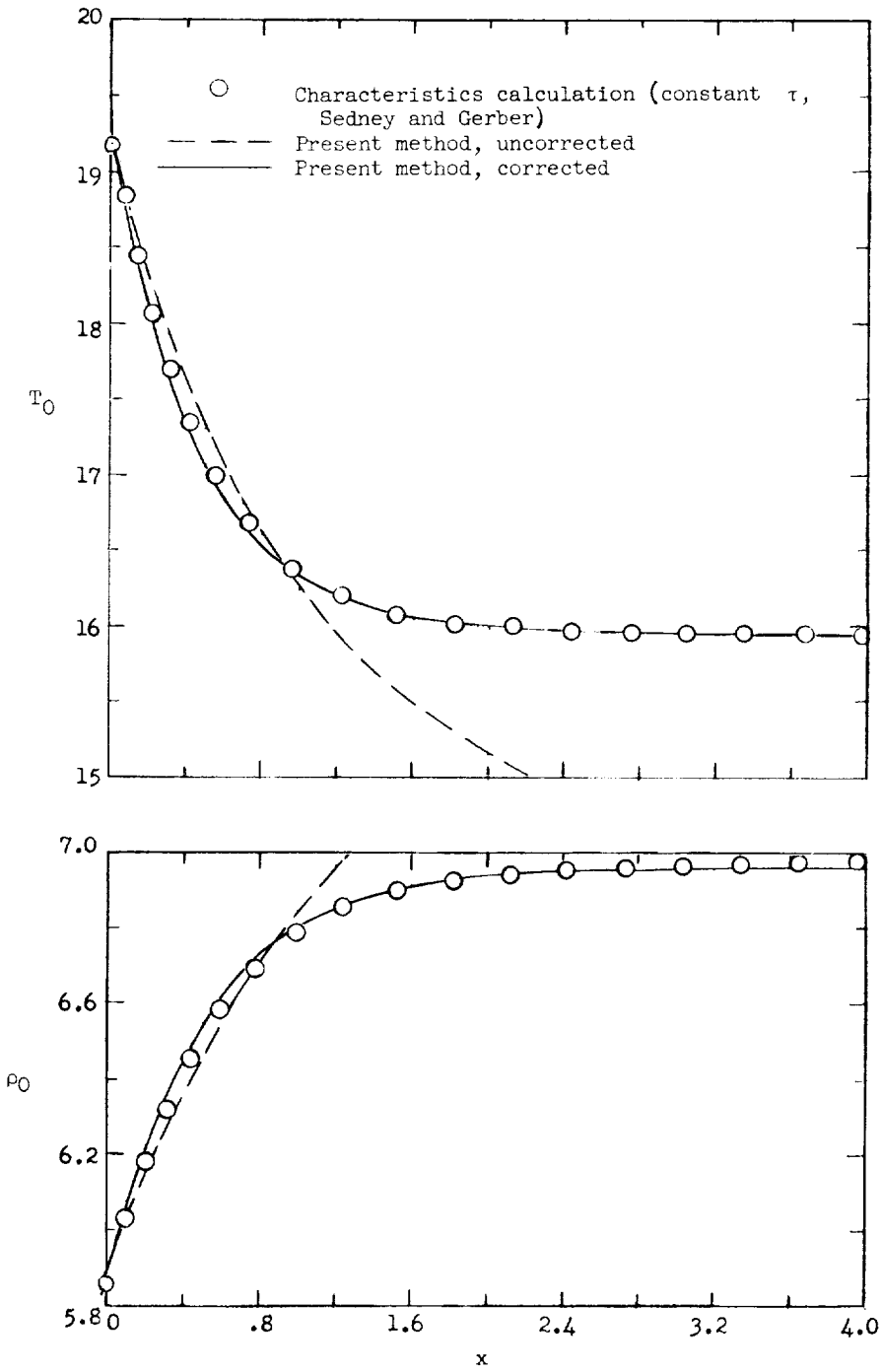

(c) Temperature and density on surface.

Figure 5.- Concluded.

in the case of the cone. In reference 2 it was noted that a good starting solution would be helpful in computing such cone flows with the method of characteristics.

Streamlines and profiles of temperature and energy.- As explained previously, the first-approximation streamline pattern, equation (55), can be used with the approximate algebraic solution of reference 1 to obtain T and E on any given streamline, allowing the construction of profiles of these variables across the shock layer. This calculation was made at two stations, $x = 4$ and 8, in each of the two numerical examples presented in figures 4 and 5. In the case of the wedge (fig. 4) the approximate streamlines were nearly straight, whereas the cone streamlines had more visible curvature, as would be expected. For illustration, several of the cone streamlines are plotted in figure 6 out to $x = 4$ for the case presented in figure 5.

The resulting profiles of T and E are shown for the wedge and cone in figures 7 and 8, respectively. Also shown in these figures are the available T-profiles taken from references 1 and 2, which resulted from variable τ calculations. The effect of variable τ is to slow the approach to equilibrium along a streamline, although the same asymptotes (as for constant τ) are reached. Since all of the present calculations were carried out for τ = Constant, a direct comparison cannot be made between the present T-profiles and those of references 1 and 2. It should be noted that, if desired, the present first approximation can be easily extended to include a variation in $\tau(p,T)$ similar to that of references 1 and 2. The approximate stream function (eq. (55)) remains unchanged, although the calculated streamline pattern would be altered slightly by the variable τ results for $\beta(x)$ and $t_0(x)$. The approximate solution for T and E can be used to include $\tau = \tau(p,T)$ and a variation in dE_{eq}/dT by restricting the simplifying assumptions to constant velocity along a streamline. Then equations (4) and (5) can be numerically integrated along a given streamline, independent of the motion equations (ref. 2).

The present approximation shows, at least qualitatively, the behavior of T and E in the interior flow. Three zones are evident in figures 7 and 8: (1) the relaxation zone behind the shock wave (ref. 17), (2) the equilibrium zone in the interior flow, and (3) the entropy layer next to the surface (refs. 1 and 2). As the distance from the tip is increased from $x = 4$ to $x = 8$, the "spreading" of the equilibrium zone is clearly discernible.

Singularities and limitations of the method.- The present method contains a sonic singularity in equations (30) to (33) just as in the ideal-gas, blunt-body problems already studied with the integral method (for example, refs. 10, 11, and 12). In the blunt-body problem, unknown initial parameters can be adjusted to satisfy the sonic condition on each strip boundary; that is, the flow must pass smoothly across the sonic line or point (unless the sonic point on the surface lies at an abrupt turn of the boundary). In the present formulation for pointed bodies with attached shocks, the initial value problem is completely determined when the flow variables at the tip can be expressed as Taylor series expansions. There are no initial parameters to adjust in order to allow a smooth transition from subsonic to supersonic flow along the surface (and along intermediate strips in higher approximations). In the limited region where the shock

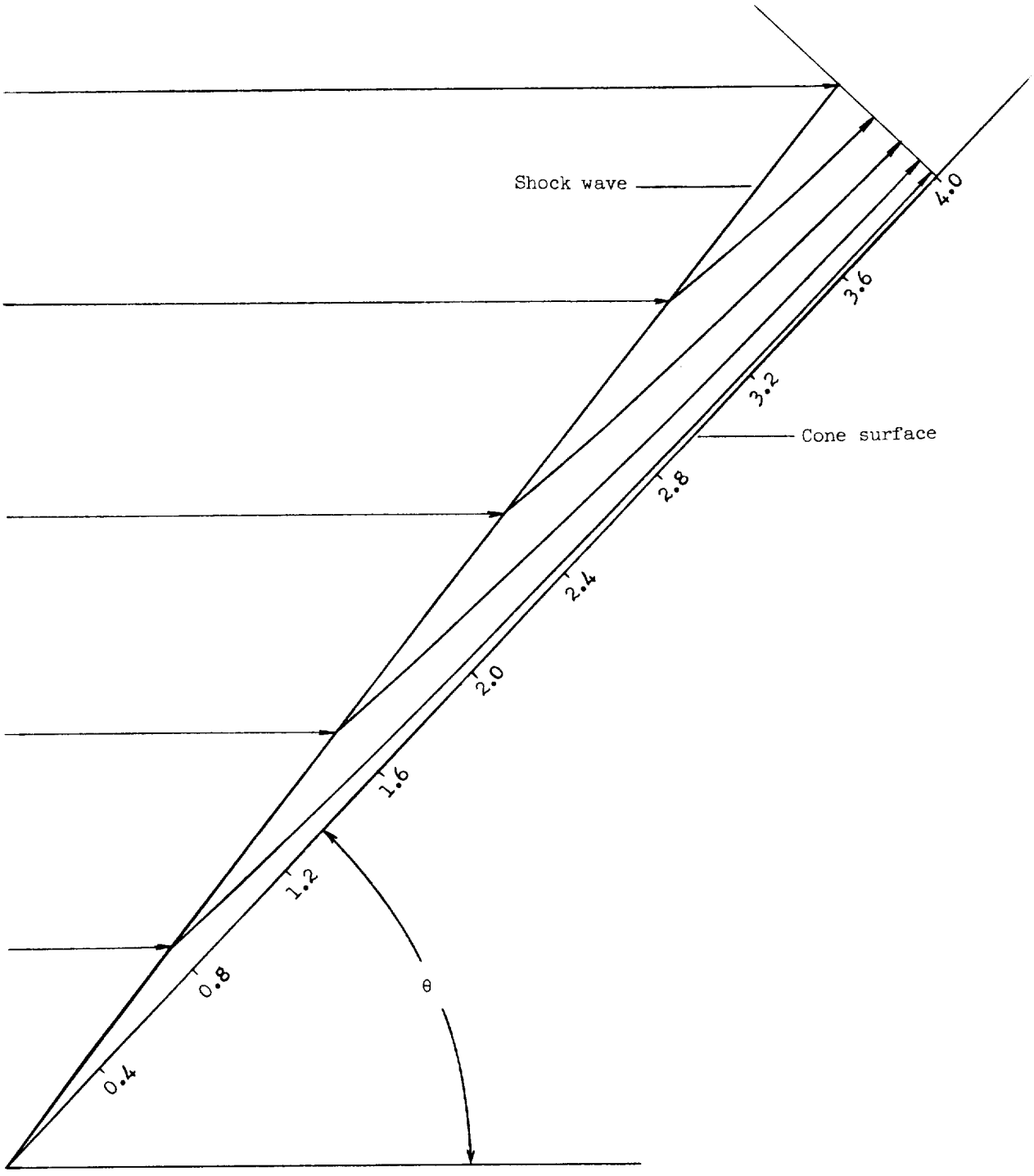

Figure 6.- Approximate streamlines for a cone in nonequilibrium vibrational flow. $M_\infty = 12$; $\theta = 46.358°$; $\Theta_v = 11.12$ (nitrogen, $T_\infty' = 300°$ K).

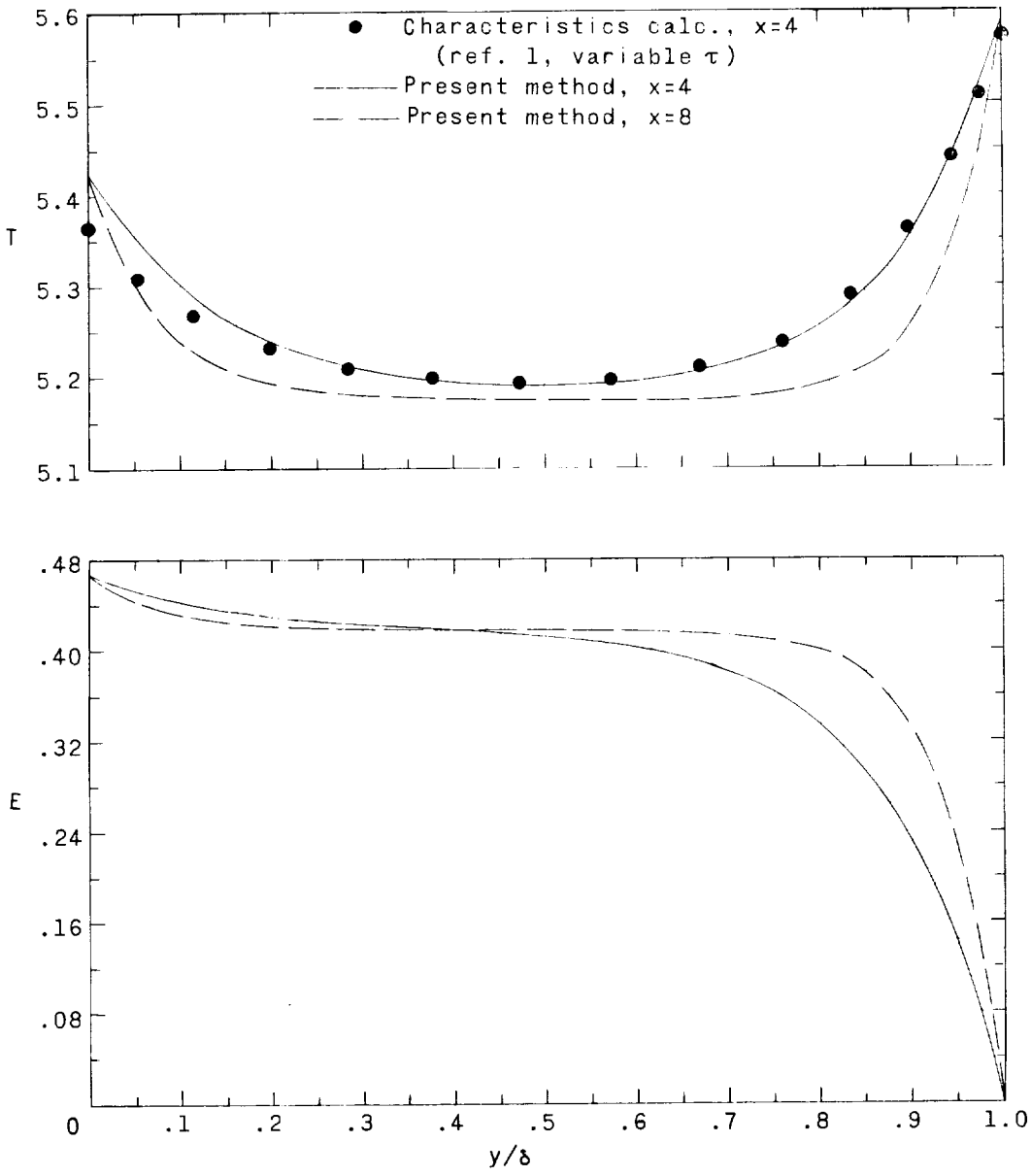

Figure 7.- Temperature and vibrational energy profiles in the shock layer of a wedge. $M_\infty = 6$; $\theta = 40.024^\circ$; $\Theta_v = 11.12$ (nitrogen, $T_\infty' = 300^\circ$ K).

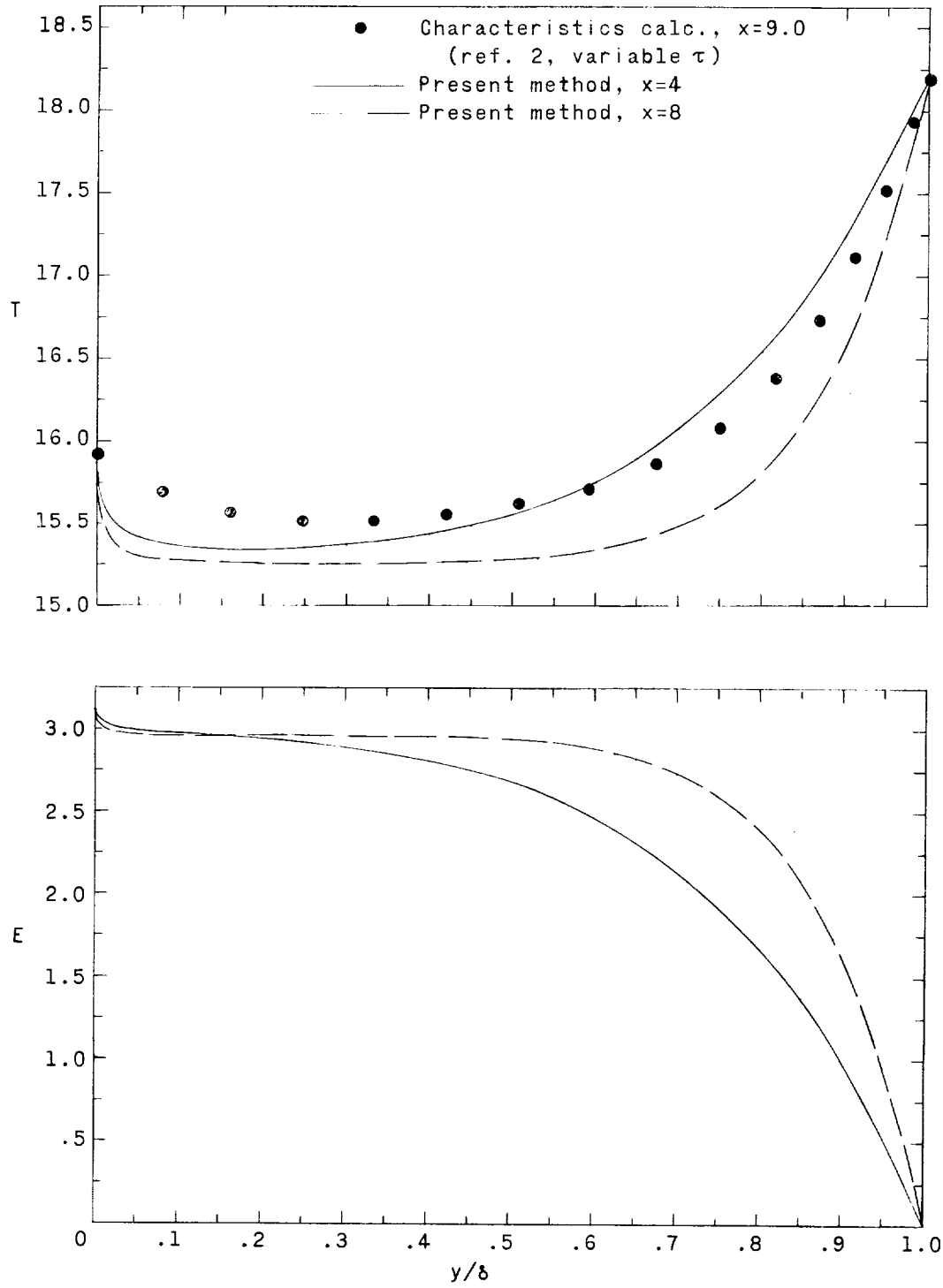

Figure 8.- Temperature and vibrational energy profiles in shock layer of a cone. $M_\infty = 12$; $\theta = 46.358^\circ$; $\Theta_v = 11.12$ (nitrogen, $T_\infty' = 300^\circ$ K).

wave is still attached, but subsonic flow exists behind the wave, it has been shown that for the wedge the Taylor series representation for the flow variables near the tip is not correct (refs. 19 and 20). This singular behavior is independent of the nonequilibrium effects. The (exact) wedge tip gradients become infinite at the "Crocco point" (ref. 20), where the denominator of J (eq. (39)) passes through zero. The Crocco point occurs at a shock-wave angle lying between the angle which gives sonic flow on the wedge surface and the detachment angle. A similar behavior is found in the present approximate expressions for the cone tip gradients. Figure 9 helps to illustrate this point. The initial derivative of the cone shock-wave angle is plotted against the initial shock-wave angle for $M_\infty = 10$ in nitrogen ($T_\infty' = 300^\circ$ K, $\Theta_V = 11.12$). It is seen that $(d\beta/dx)_{x=0}$ becomes increasingly negative as the subsonic region is entered, reversing sign ahead of the detachment angle. This phenomenon for the cone appears to be the axisymmetric analog to the Crocco point singularity in the plane, attached-shock flows.

Numerical integration of the present differential equations became increasingly unstable as the initial shock-wave angle approached that which gives frozen-flow sonic velocity on the cone surface. The present method was incapable of computing a case handled successfully in reference 2; namely, $M_\infty = 10$, $\beta_{x=0} = 64.50^\circ$, $\theta = 53.82^\circ$. For this case the initial frozen-flow Mach number on the cone surface is about 1.07.

It is believed that most of the basic procedures applied in the present paper will carry over to problems with more complex thermodynamics. The presence of several time or length scales (for example, coupled relaxation processes, surface curvature, etc.) may present difficulties, but no more so than with other methods. The use of the integral method in nonequilibrium, mixed flows with detached shock waves should give useful results, in light of the present analysis and previous successes of the method in ideal-gas mixed flows.

CONCLUDING REMARKS

The method of integral relations was used to calculate the vibrationally relaxing flow of a pure diatomic gas over wedges and cones. The first (one-strip) approximation was used to convert the exact partial differential equations to an approximate set of ordinary equations, which were numerically integrated by standard procedures.

1. In order to obtain a workable solution, integration of all of the partial differential equations across the shock layer was necessary, and then corrections consistent with the surface momentum and rate equations had to be applied. In previous applications to ideal-gas, blunt-body problems, and in certain conical-flow problems, one of the differential momentum equations was omitted and replaced by an algebraic equation (the isentropic law).

2. The present approximate results for nonequilibrium flow past wedges and cones were in excellent agreement near the tip with other calculations obtained

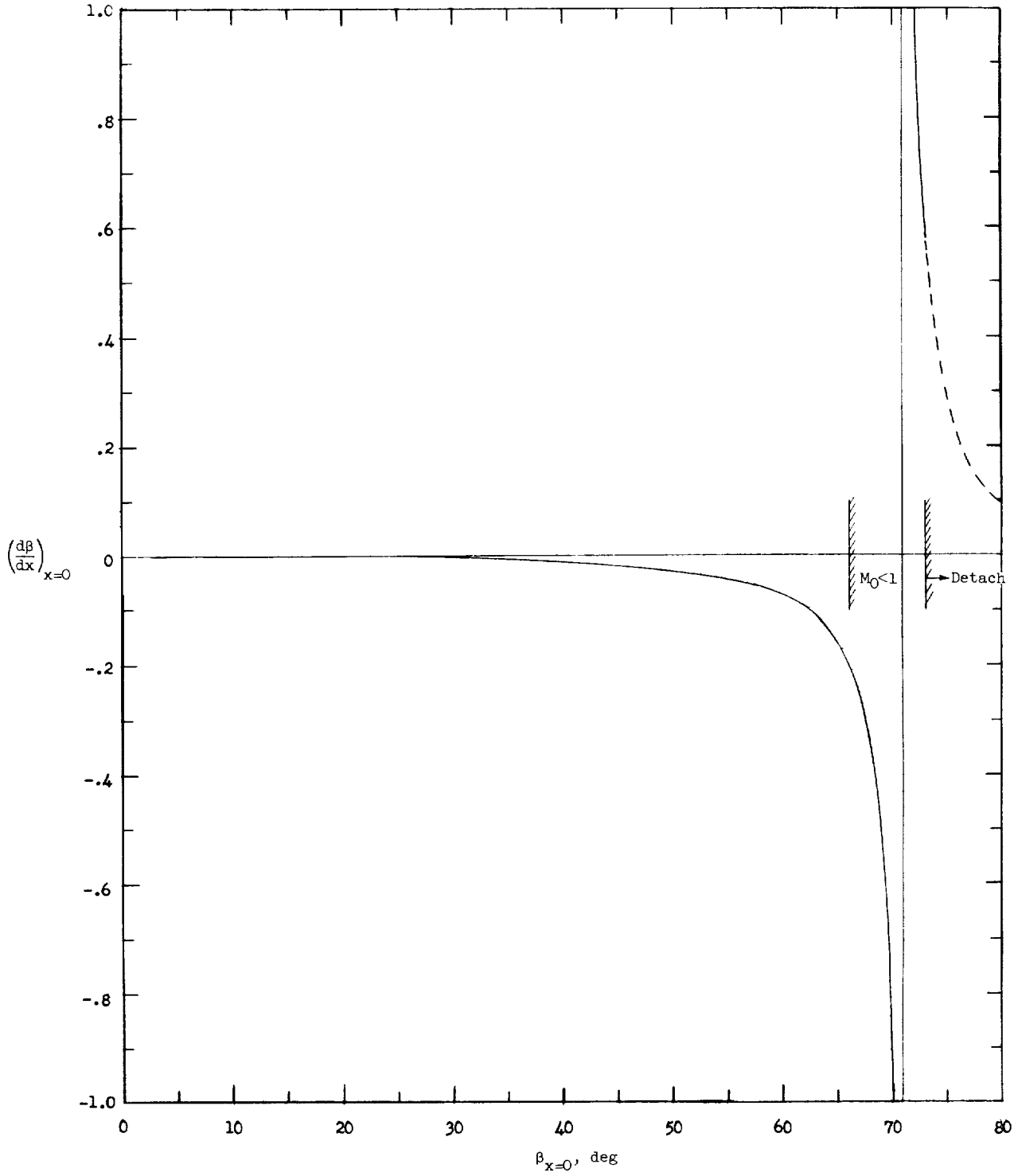

Figure 9.- Initial shock-wave angle derivative as function of initial shock-wave angle for a cone. $M_\infty = 10$; $\Theta_v = 11.12$ (nitrogen, $T_\infty' = 300^\circ$ K).

by the exact numerical method of characteristics. At large distances from the tip, the correct asymptotes were not reached, but the error was not great. In view of the previously demonstrated rapid convergence of higher approximations in ideal-gas, mixed-flow problems, the second approximation should yield more accurate results at large distances with little additional computer time.

3. Since the linear profiles of the first approximation do not give realistic details within the shock layer, an approximate stream function was given in closed form and was used to construct profiles of temperature and vibrational energy across the shock layer at any distance from the tip. In the case of frozen or equilibrium cone flow, the approximate streamlines were hyperbolas, a result obtained previously by a somewhat different approach.

4. The present approximate differential equations reduced to an algebraic system in the special cases of frozen or equilibrium flow. This solution for the cone was found to be in good agreement with the exact solutions for both frozen and vibrational equilibrium flow.

5. The method is limited in the present formulation to cases where the flow in the shock layer is entirely supersonic. The approximate differential equations contain a singularity when the surface velocity is sonic, and there are no initial parameters to adjust in order to surmount this difficulty.

Langley Research Center,
National Aeronautics and Space Administration,
Langley Station, Hampton, Va., May 17, 1963.

APPENDIX A

DERIVATION OF THE FIRST INTEGRAL APPROXIMATION

The ordinary differential equations of the first integral approximation are obtained by integrating equations (10) to (13) across the shock layer from $y = 0$ to $y = \delta$. The following notation is helpful:

$f_0 = f_0(x)$ = Any variable or product of variables at the surface ($y = 0$)

$f_\delta = f_\delta(x)$ = Any variable or product of variables just behind the shock wave ($y = \delta$)

In this one-strip approximation, linear profiles are used; for example,

$$f(x,y) = f_0 + \left(f_\delta - f_0\right)\frac{y}{\delta} \tag{A1}$$

and

$$\int_0^\delta f(x,y)dy = \frac{\delta}{2}\left(f_0 + f_\delta\right) \tag{A2}$$

Leibnitz's rule for differentiation under the integral sign is applied as follows:

$$\int_0^\delta \frac{\partial}{\partial x}\left[f(x,y)\right]dy = \frac{d}{dx}\int_0^\delta f(x,y)dy - f_\delta \frac{d\delta}{dx} \tag{A3}$$

Substituting equations (A2) and (15) into equation (A3) gives

$$\int_0^\delta \frac{\partial}{\partial x}\left[f(x,y)\right]dy = \frac{\delta}{2}\frac{df_0}{dx} + \frac{\delta}{2}\frac{df_\delta}{dx} + \frac{1}{2}\left(f_0 - f_\delta\right)\tan\lambda \tag{A4}$$

Also needed are the relations

$$\left.\begin{aligned} r_0 &= x \sin\theta \\ r_\delta &= x \sin\theta + \delta \cos\theta \end{aligned}\right\} \tag{A5}$$

Then integration of equations (10) to (13) from $y = 0$ to $y = \delta$ is straightforward, and equations (16) to (19) are obtained with the help of equations (A1) to (A5), the boundary conditions (14a) and (14b), and division by $x \sin\theta$. Finally, the substitution $\phi = \frac{\delta}{x}$ is made.

APPENDIX B

APPROXIMATE SOLUTION FOR VIBRATIONAL EQUILIBRIUM CONE FLOW

Vibrational equilibrium cone flow can be calculated with the present method as follows:

(1) The values of M_∞, Θ_v, and ω (or β) are given

(2) The conservation of mass and momentum across an oblique shock wave can be expressed as follows:

$$\rho_\delta V_\delta = \frac{\sin \beta}{\sin(\beta - \omega)} \tag{B1}$$

$$p_\delta + \rho_\delta V_\delta^2 \sin^2(\beta - \omega) = \frac{5}{7M_\infty^2} + \sin^2\beta \tag{B2}$$

$$V_\delta = \frac{\cos \beta}{\cos(\beta - \omega)} \tag{B3}$$

Equations (B1), (B2), and (B3) can be combined with the perfect-gas equation of state (eq. (6) of main text) to yield:

$$T_\delta = \mu(1 + 7B) \tag{B4}$$

where

$$\mu = \tan(\beta - \omega)\cot \beta \tag{B5}$$

and

$$B = \frac{M_\infty^2}{5} \sin^2\beta(1 - \mu) \tag{B6}$$

The energy equation (on the assumption that $E_\infty = 0$) is

$$T_\delta + E_\delta = 1 + B(1 + \mu) \tag{B7}$$

where

$$E_\delta = E_{eq,\delta} = \frac{2}{7} \Theta_v \left[\exp\left(\frac{\Theta_v}{T_\delta}\right) - 1\right]^{-1} \tag{B8}$$

If ω (or β) has been prescribed, equations (B4) to (B8) must be solved by trial and error by choosing β (or ω) until the T_δ obtained from equation (B4) satisfies equation (B7). When the desired accuracy is obtained, V_δ is obtained from equation (B3), while

$$p_\delta = \frac{5}{7M_\infty{}^2}(1 + 7B) \tag{B9}$$

and

$$\rho_\delta = \frac{1}{\mu} \tag{B10}$$

(3) The cone angle θ must now be determined by trial and error from equations (23), (25), (26), (5), (6), and (8):

$$u_0 = V_\delta \cos(\theta - \omega)\left[1 - \frac{\tan(\theta - \omega)}{2 \cot \lambda + \cot \theta}\right] \tag{B11}$$

$$p_0 = p_\delta + 2\left(\frac{\cot \lambda + \cot \theta}{2 \cot \lambda + \cot \theta}\right)\rho_\delta V_\delta{}^2 \sin^2(\theta - \omega) \tag{B12}$$

$$T_0 + E_0 = 1 + \frac{M_\infty{}^2}{5}\left(1 - u_0{}^2\right) \tag{B13}$$

$$E_0 = E_{eq,0} = \frac{2}{7}\,\Theta_v\left[\exp\left(\frac{\Theta_v}{T_0}\right) - 1\right]^{-1} \tag{B14}$$

$$\rho_0 = \frac{7}{5}\,M_\infty{}^2\,\frac{p_0}{T_0} \tag{B15}$$

$$\rho_0 u_0 = (\cot \lambda + \cot \theta)\rho_\delta V_\delta \sin(\theta - \omega) \tag{B16}$$

APPENDIX C

COEFFICIENTS IN EQUATIONS (30) TO (33)

The coefficients in equations (30) to (33) are:

$$A_{11} = \frac{7}{5} M_0^2 \tag{C1}$$

$$A_{12} = \frac{u_0 t_0}{T_0} \tag{C2}$$

$$A_{13} = \left(1 + \frac{2}{5} M_0^2\right) t_0 \tag{C3}$$

$$A_{14} = \left(1 + j\phi \cot \theta\right) u_0 \frac{dt_\delta}{d\beta} \tag{C4}$$

$$A_{21} = 1 + \frac{7}{5} M_0^2 \tag{C5}$$

$$A_{22} = \frac{u_0 t_0}{T_0} \tag{C6}$$

$$A_{23} = \left(2 + \frac{2}{5} M_0^2\right) t_0 \tag{C7}$$

$$A_{24} = \left(1 + j\phi \cot \theta\right) \frac{dg_\delta}{d\beta} \tag{C8}$$

$$A_{34} = \left(1 + j\phi \cot \theta\right) \frac{dz_\delta}{d\beta} \tag{C9}$$

$$A_{41} = \frac{7}{5} M_0^2 E_0 \tag{C10}$$

$$A_{42} = u_0 t_0 \left(1 + \frac{E_0}{T_0}\right) \tag{C11}$$

$$A_{43} = \left(1 + \frac{2}{5} M_0^2\right) t_0 E_0 \tag{C12}$$

$$K_1 = -\frac{u_0}{x\phi}\left\{(\tan\lambda + j\phi)t_0 - (\tan\lambda - j\phi)t_\delta + 2(1 + j\phi\cot\theta)h_\delta\right\} \tag{C13}$$

$$K_2 = -\frac{1}{x\phi}\left\{(\tan\lambda + j\phi)u_0t_0 - (\tan\lambda - j\phi)u_\delta t_\delta + 2(1 + j\phi\cot\theta)z_\delta + \tan\lambda\left(p_0 - p_\delta\right)\right\} \tag{C14}$$

$$K_3 = -\frac{1}{x\phi}\left\{-(\tan\lambda - j\phi)z_\delta + 2(1 + j\phi\cot\theta)v_\delta h_\delta - (2 + j\phi\cot\theta)\left(p_0 - p_\delta\right)\right\} \tag{C15}$$

$$K_4 = -\frac{u_0}{x\phi}\left\{(\tan\lambda + j\phi)t_0E_0 - x\phi\left[\rho_0\epsilon_0 + (1 + j\phi\cot\theta)\rho_\delta\epsilon_\delta\right]\right\} \tag{C16}$$

APPENDIX D

FROZEN SHOCK-WAVE RELATIONS

The frozen shock-wave relations needed throughout this work are given below for $\gamma = 7/5$ (ref. 15):

Define

$$m(\beta, M_\infty) = M_\infty^2 \sin^2\beta \tag{D1}$$

$$a(\beta, M_\infty) = \frac{5}{6M_\infty^2}(m - 1) \tag{D2}$$

Then

$$u_\delta = (1 - a)\cos\theta + a \cot\beta \sin\theta \tag{D3}$$

$$v_\delta = -(1 - a)\sin\theta + a \cot\beta \cos\theta \tag{D4}$$

$$\rho_\delta = \frac{6m}{5 + m} \tag{D5}$$

$$p_\delta = \frac{35m - 5}{42M_\infty^2} \tag{D6}$$

$$\frac{du_\delta}{d\beta} = -\frac{5}{3}\cos\beta \sin\lambda - \frac{a \sin\theta}{\sin^2\beta} \tag{D7}$$

$$\frac{dv_\delta}{d\beta} = \frac{5}{3}\cos\beta \cos\lambda - \frac{a \cos\theta}{\sin^2\beta} \tag{D8}$$

$$\frac{d\rho_\delta}{d\beta} = \frac{60m \cot\beta}{(5 + m)^2} \tag{D9}$$

$$\frac{dp_\delta}{d\beta} = \frac{5}{3}\sin\beta \cos\beta \tag{D10}$$

From these equations other shock-wave quantities can easily be calculated, for example:

$$z_\delta = \rho_\delta u_\delta v_\delta = t_\delta v_\delta$$

and

$$\frac{dz_\delta}{d\beta} = t_\delta \frac{dv_\delta}{d\beta} + v_\delta \frac{dt_\delta}{d\beta} = t_\delta \frac{dv_\delta}{d\beta} + v_\delta \left(u_\delta \frac{d\rho_\delta}{d\beta} + \rho_\delta \frac{du_\delta}{d\beta} \right)$$

APPENDIX E

DEFINITIONS OF SYMBOLS APPEARING IN EQUATIONS (40) TO (43)

The following notation is introduced as a means of simplifying equations (40) to (43):

$$K = \frac{1}{3}\frac{u_0}{T_0}\left[\rho_0\epsilon_0 + (1 + \tan\lambda\cot\theta)\rho_\delta\epsilon_\delta\right] \tag{E1}$$

$$L = -\left(1 + \frac{2}{5}M_0^2\right)\left[\frac{2}{3}F_3 - (2\cot\lambda + \cot\theta)\left(F_1 - F_2\right)\right]$$

$$+ \frac{7}{5}M_0^2F_3 + (2\cot\lambda + \cot\theta)F_1 \tag{E2}$$

$$F_1 = \frac{u_0}{3}\left\{(\cot\lambda + \cot\theta)\left(\tan\lambda\frac{dt_\delta}{d\beta} + 2\frac{dh_\delta}{d\beta}\right) + \csc 2\lambda\left(3t_0 - t_\delta + 2\cot\theta\, h_\delta\right)\right\} \tag{E3}$$

$$F_2 = \frac{1}{3}\left\{(\cot\lambda + \cot\theta)\left[\tan\lambda\frac{d}{d\beta}(u_\delta t_\delta) + 2\frac{dz_\delta}{d\beta}\right] + \tan\lambda\cot\theta\frac{dp_\delta}{d\beta}\right.$$

$$\left. + \csc 2\lambda\left[3u_0t_0 - u_\delta t_\delta + 2\cot\theta\, z_\delta + 2\left(p_0 - p_\delta\right)\right]\right\} \tag{E4}$$

$$F_3 = (\cot\lambda + \cot\theta)\left[\tan\lambda\frac{dz_\delta}{d\beta} + 2\frac{d}{d\beta}\left(v_\delta h_\delta\right)\right] + (2\cot\lambda + \cot\theta)\frac{dp_\delta}{d\beta}$$

$$+ \csc 2\lambda\left[-z_\delta + 2\cot\theta\, v_\delta h_\delta - \cot\theta\left(p_0 - p_\delta\right)\right] \tag{E5}$$

REFERENCES

1. Sedney, R., South, J. C., and Gerber, N.: Characteristic Calculation of Nonequilibrium Flows. Rep. No. 1173, Ballistics Res. Lab., Aberdeen Proving Ground, Apr. 1962.

2. Sedney, R., and Gerber, N.: Nonequilibrium Flow Over a Cone. IAS Paper No. 63-71, Inst. Aerospace Sci., Jan. 1963.

3. Van Dyke, M. D.: The Supersonic Blunt-Body Problem - Review and Extension. Jour. Aero/Space Sci., vol. 25, no. 8, Aug. 1958, pp. 485-496.

4. Hayes, Wallace D., and Probstein, Ronald F.: Hypersonic Flow Theory. Academic Press, Inc. (New York), 1959.

5. Lick, W.: Inviscid Flow Around a Blunt Body of a Reacting Mixture of Gases - Part A. General Analysis. TR AE 5810 (AFOSR TN-58-522, AD No. 158 335), Rensselaer Polytechnic Inst., May 1958.

6. Lick, W. J.: Inviscid Flow Around a Blunt Body of a Reacting Mixture of Gases - Part B. Numerical Solutions. TR AE 5814 (AFOSR TN-58-1124, AD 207883), Rensselaer Polytechnic Inst., Dec. 1958.

7. Dorodnicyn, A. A.: A Contribution to the Solution of Mixed Problems of Transonic Aerodynamics. Advances in Aeronautical Sciences, Vol. 2, Pergamon Press, 1959, pp. 832-844.

8. Traugott, Stephen C.: Some Features of Supersonic and Hypersonic Flow About Blunted Cones. Jour. Aerospace Sci., vol. 29, no. 4, Apr. 1962, pp. 389-399.

9. Holt, Maurice: Direct Calculation of Pressure Distribution on Blunt Hypersonic Nose Shapes With Sharp Corners. Jour. Aerospace Sci., vol. 28, no. 11, Nov. 1961, pp. 872-876.

10. Belotserkovskii, O. M.: Flow With a Detached Shock Wave About a Symmetrical Profile. Jour. Applied Mathematics and Mechanics, vol. 22, no. 2, Pergamon Press, Inc., 1958, pp. 279-298. (Translation of Prikladnaia Matematika I Mekhanika.)

11. Traugott, Stephen C.: An Approximate Solution of the Direct Supersonic Blunt-Body Problem for Arbitrary Axisymmetric Shapes. Jour. Aerospace Sci., vol. 27, no. 5, May 1960, pp. 361-370.

12. Gold, Ruby, and Holt, Maurice: Calculation of Supersonic Flow Past a Flat-Headed Cylinder by Belotserkovskii's Method. Div. Applied Math., Brown Univ. (AFOSR TN-59-199, AD 211-525), Mar. 1959.

13. Bethe, H. A., and Teller, E.: Deviations From Thermal Equilibrium in Shock Waves. Rep. X-117, Ballistic Res. Lab., Aberdeen Proving Ground, 1945.

14. Chushkin, P. I., and Shchennikov, V. V.: Calculation of Certain Conical Flows Without Axial Symmetry. (Raschet Nekatorykh Konicheskikh Technii Bez Osevoi Simmetrii.) Trans. No. 926, British R.A.E., Dec. 1960.

15. Ames Research Staff: Equations, Tables, and Charts for Compressible Flow. NACA Rep. 1135, 1953. (Supersedes NACA TN 1428.)

16. Kelly, Paul D.: Conical Flow Parameters for Air and Nitrogen in Vibrational Equilibrium. Rep. No. 1164, Ballistic Res. Lab., Aberdeen Proving Ground, Mar. 1962.

17. Sedney, Raymond: Some Aspects of Nonequilibrium Flows. Jour. Aerospace Sci., vol. 28, no. 3, Mar. 1961, pp. 189-196, 208.

18. Hord, Richard A.: An Approximate Solution for Axially Symmetric Flow Over a Cone With an Attached Shock Wave. NACA TN 3485, 1955.

19. Guderley, K. Gottfried: Considerations on the Structure of Mixed Subsonic-Supersonic Flow Patterns. Tech. Rep. No. F-TR-2168-ND, Air Materiel Command, U.S. Air Force, Oct. 1947.

20. Ferri, A.: Supersonic Flows With Shock Waves. General Theory of High Speed Aerodynamics. Vol. VI of High Speed Aerodynamics and Jet Propulsion, sec. H, ch. I, par. 4, W. R. Sears, ed., Princeton Univ. Press, 1954, pp. 678-683.